# Deformation due to strike-slip faults: Theory and observations

- Individual earthquakes
- Modeling of multiple earthquake cycles on fault systems

# Individual events

- Coseismic (static/dynamic?)
- Postseismic
- Interseismic

What essential physics and what constitutive laws should the models incorporate?

- 3-D variations in elastic properties
- Non-linear visco-elasticity?
- Plasticity?
- Poro-elasticity?
- Gravity
- Pre-stress
- Topography?
- Rate-and-state friction
- Temperature-dependent rheology?

## M7.3 Landers, 1992

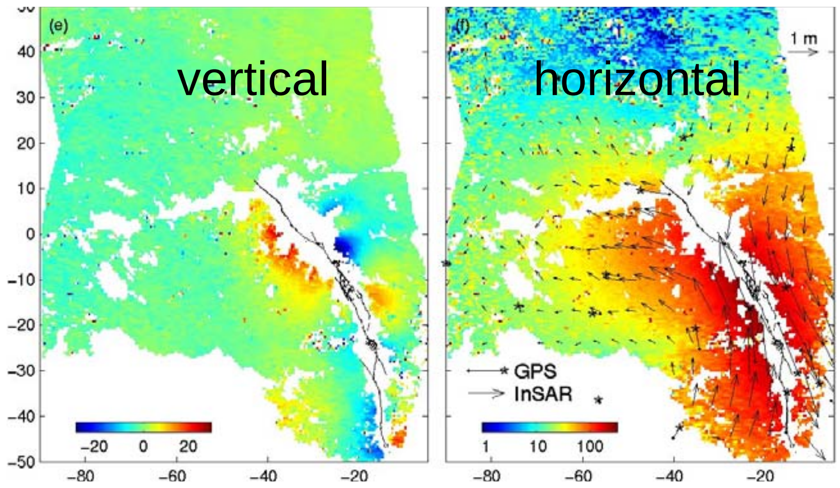


## M7.1 Hector Mine, 1999

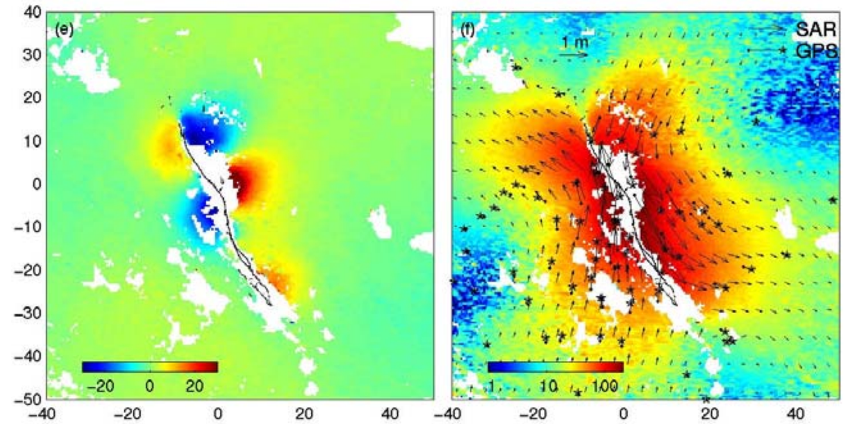


## M6.6 Bam (Iran), 2003

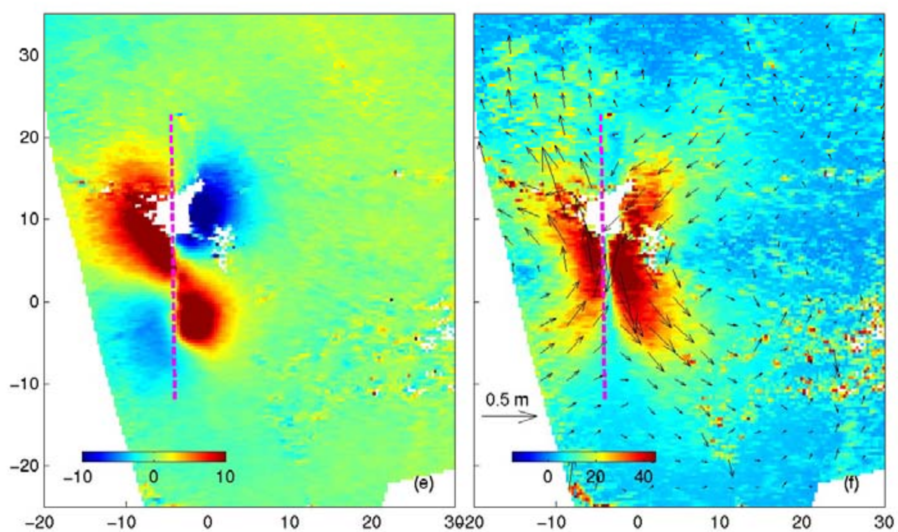


## Dislocation

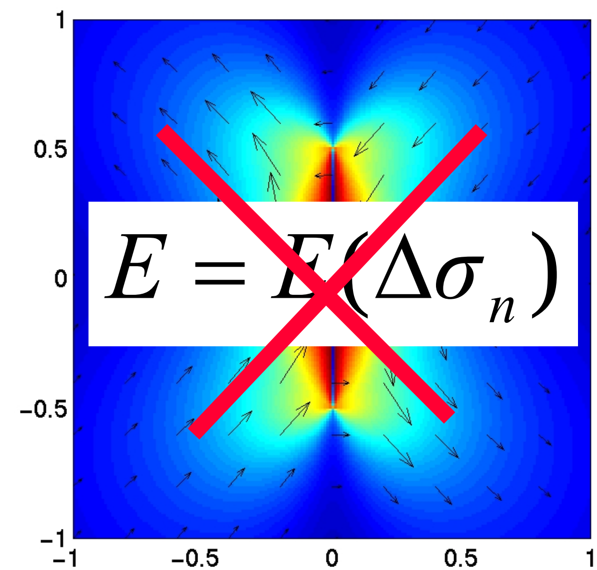

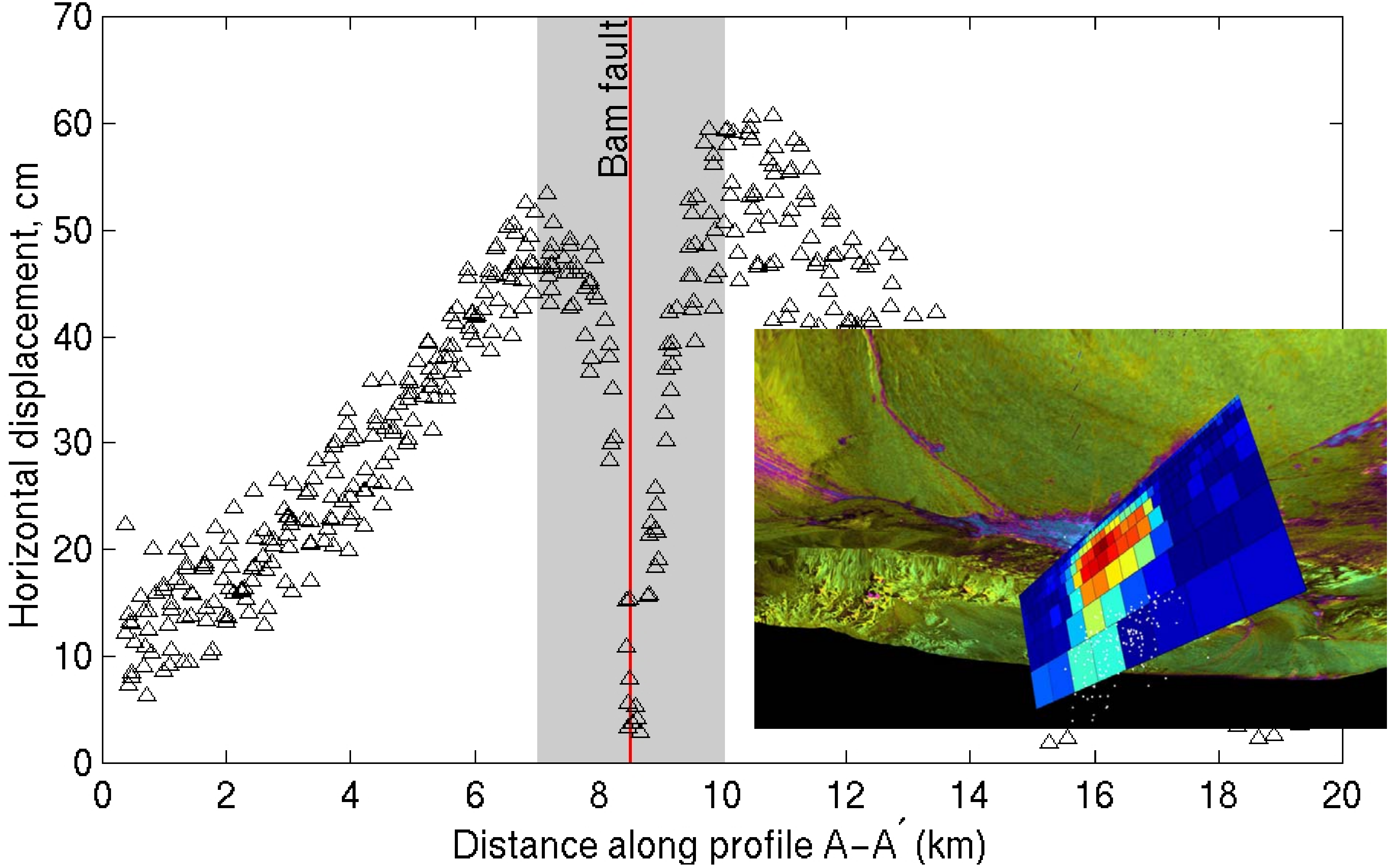
Bam fault
Horizontal displacement, cm
Distance along profile A–A′ (km)
0
10
20
30
40
50
60
70
0
2
4
6
8
10
12
14
16
18
20

# Southern San Andreas Fault

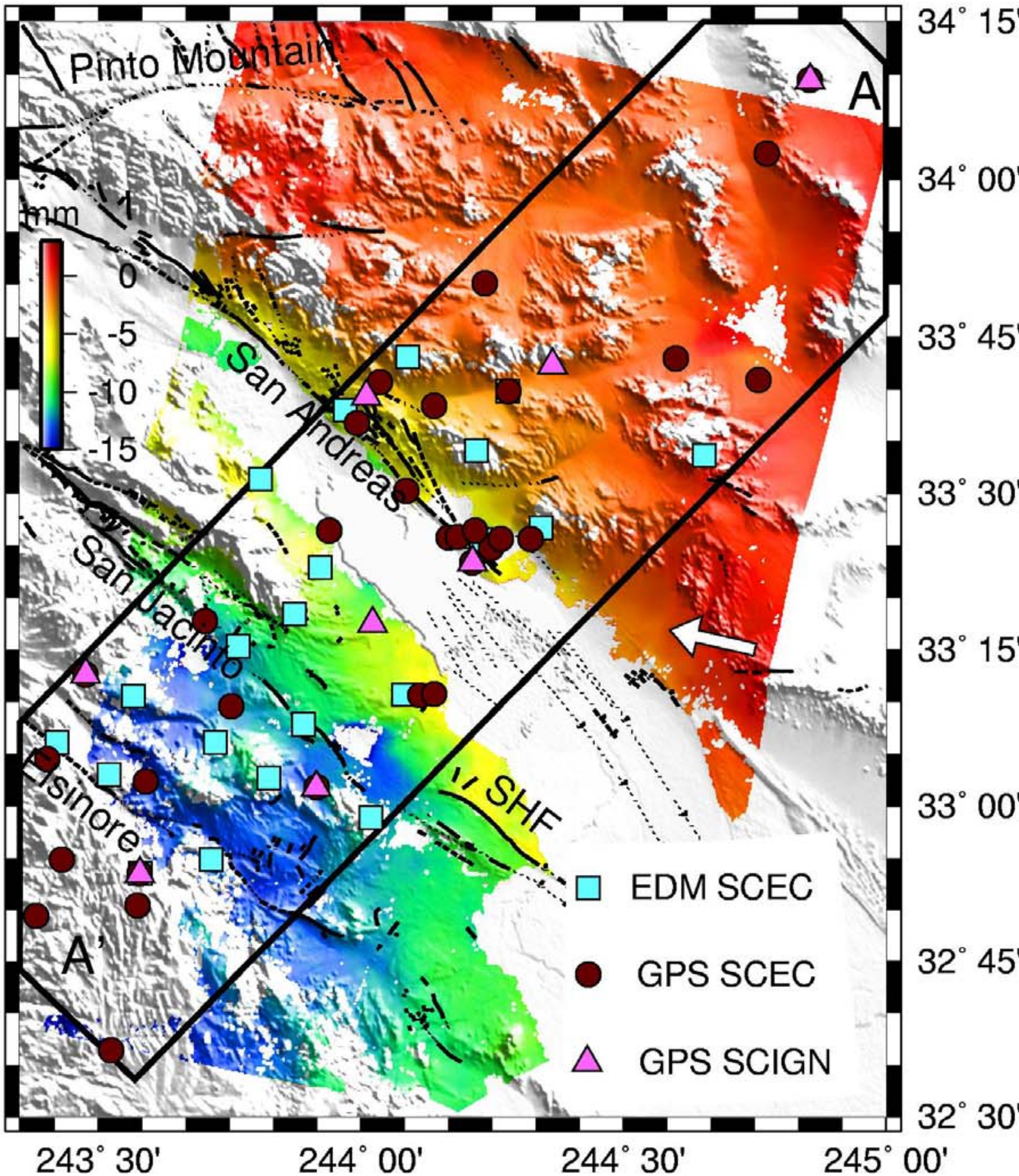


Line of sight velocities from stacked InSAR data

35 interferograms

Epoch: 1992-2000

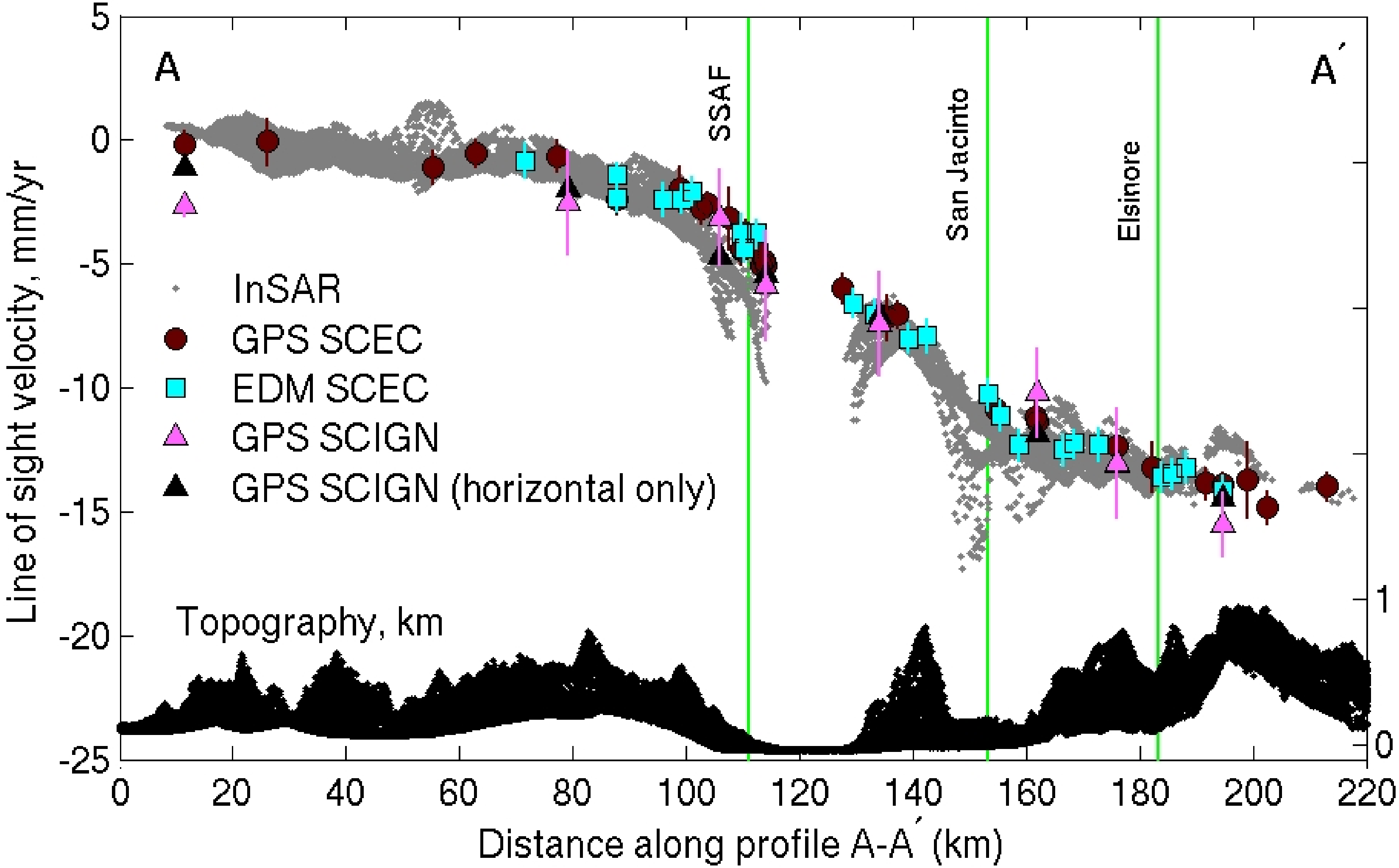

A
A´
SSAF
San Jacinto
Elsinore
InSAR
GPS SCEC
EDM SCEC
GPS SCIGN
GPS SCIGN (horizontal only)
Topography, km
Line of sight velocity, mm/yr
Distance along profile A-A´ (km)

$G_1/G_2 < 0.4$

(also, see LePichon et al., JGR 2005).

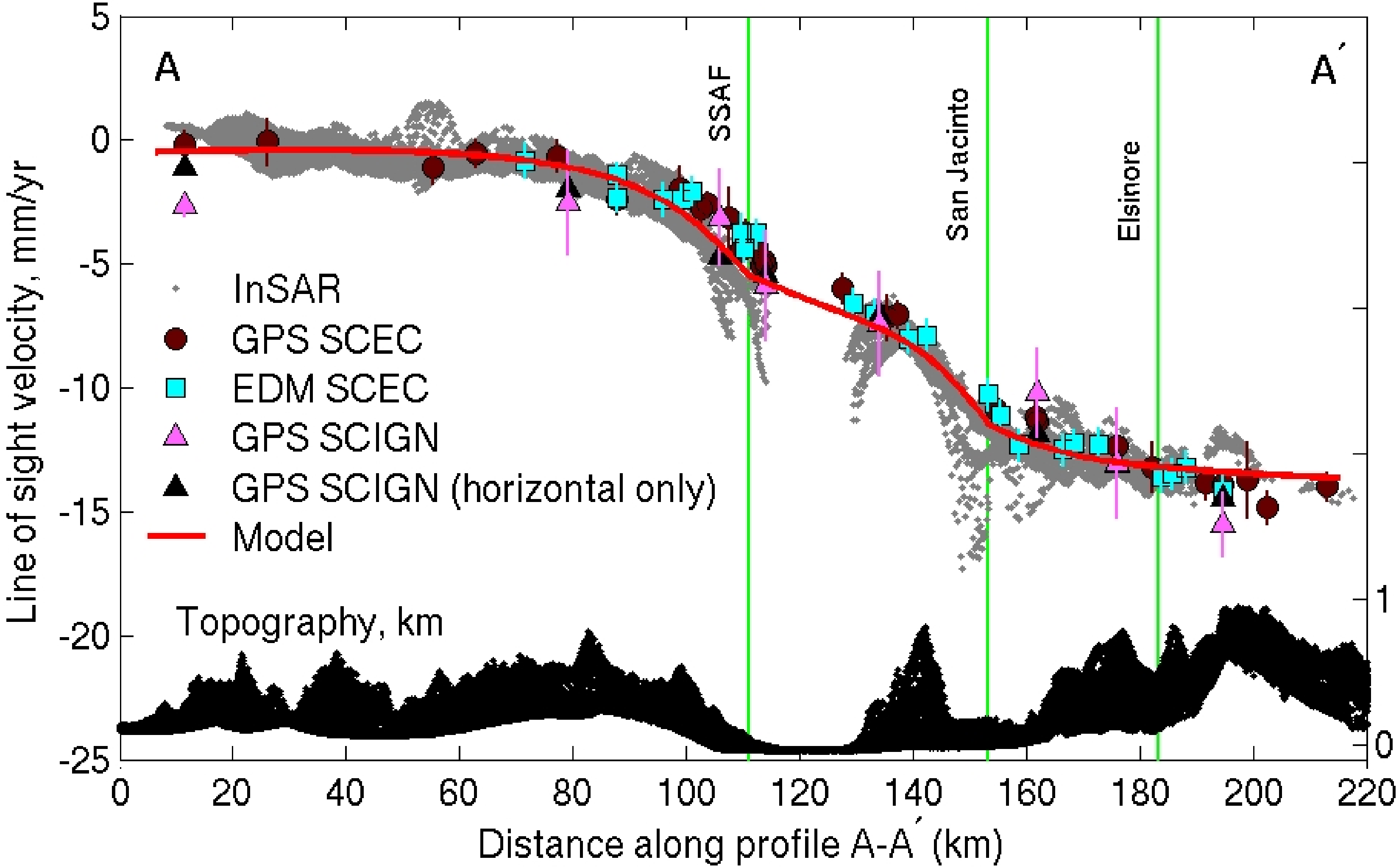

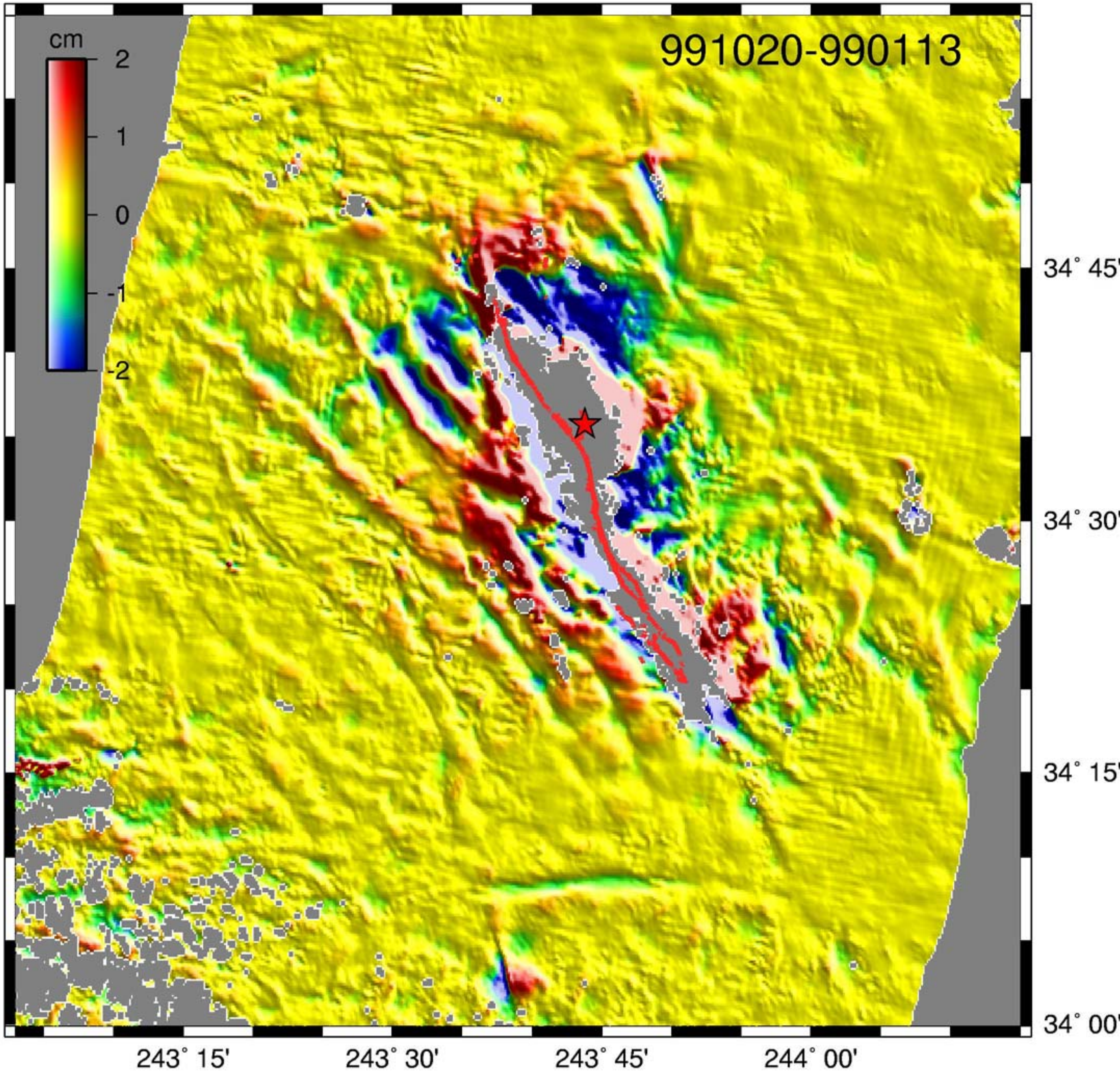
991020-990113
cm
2
1
0
-1
-2
34˚ 45'
34˚ 30'
34˚ 15'
34˚ 00'
243˚ 15'
243˚ 30'
243˚ 45'
244˚ 00'

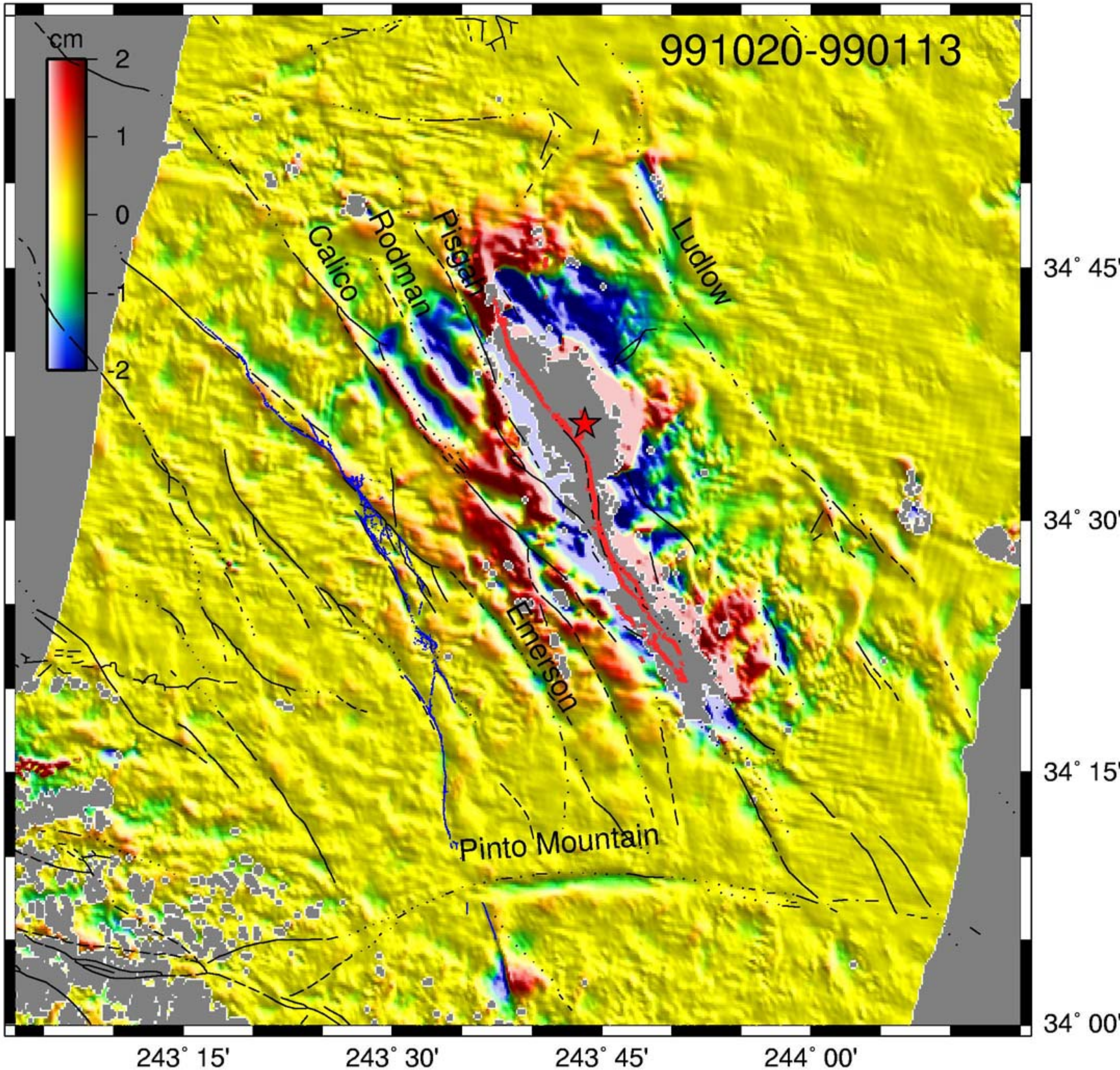

991020-990113
cm
2
1
0
-1
-2
Calico
Rodman
Pisgah
Ludlow
Emerson
Pinto Mountain
34˚ 45'
34˚ 30'
34˚ 15'
34˚ 00'
243˚ 15'
243˚ 30'
243˚ 45'
244˚ 00'

# Evidence for macroscopic low rigidity zones around major faults

- Seismic: Li et al., 1994; Eberhart-Phillips et al. 1995; Thurber et al., 1997; McGuire and Ben-Zion, 2005

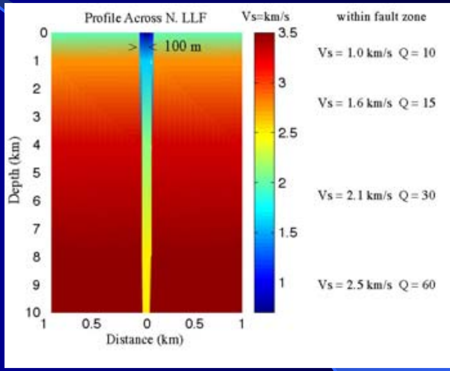


- Field: Johnson et al., 1997; Chester and Chester, 1998; Wilson et al. 2005

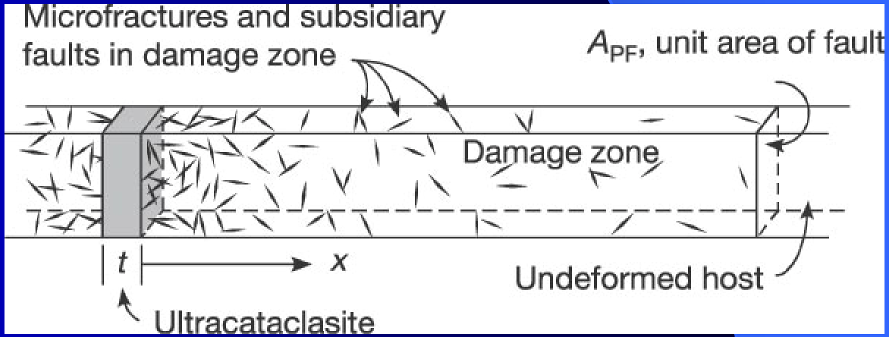


Chester et al., 2005

# Origin of compliant zones

- Damage due … gh stresses at the rupture f… on sub-parallel segments, af…
- Geometric c… aults, fault step-overs)?
- Interplay bet… -dependent healing (Vid… , … )
- How much shear strain is accommodated off the "primary slip surface"?
- Dependence on a cumulative fault slip?

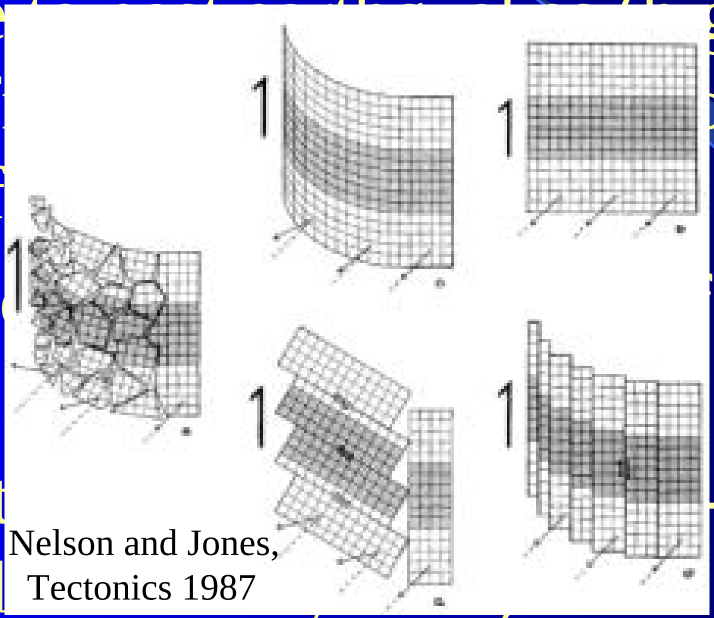

Nelson and Jones, Tectonics 1987

# Shallow coseismic slip deficit

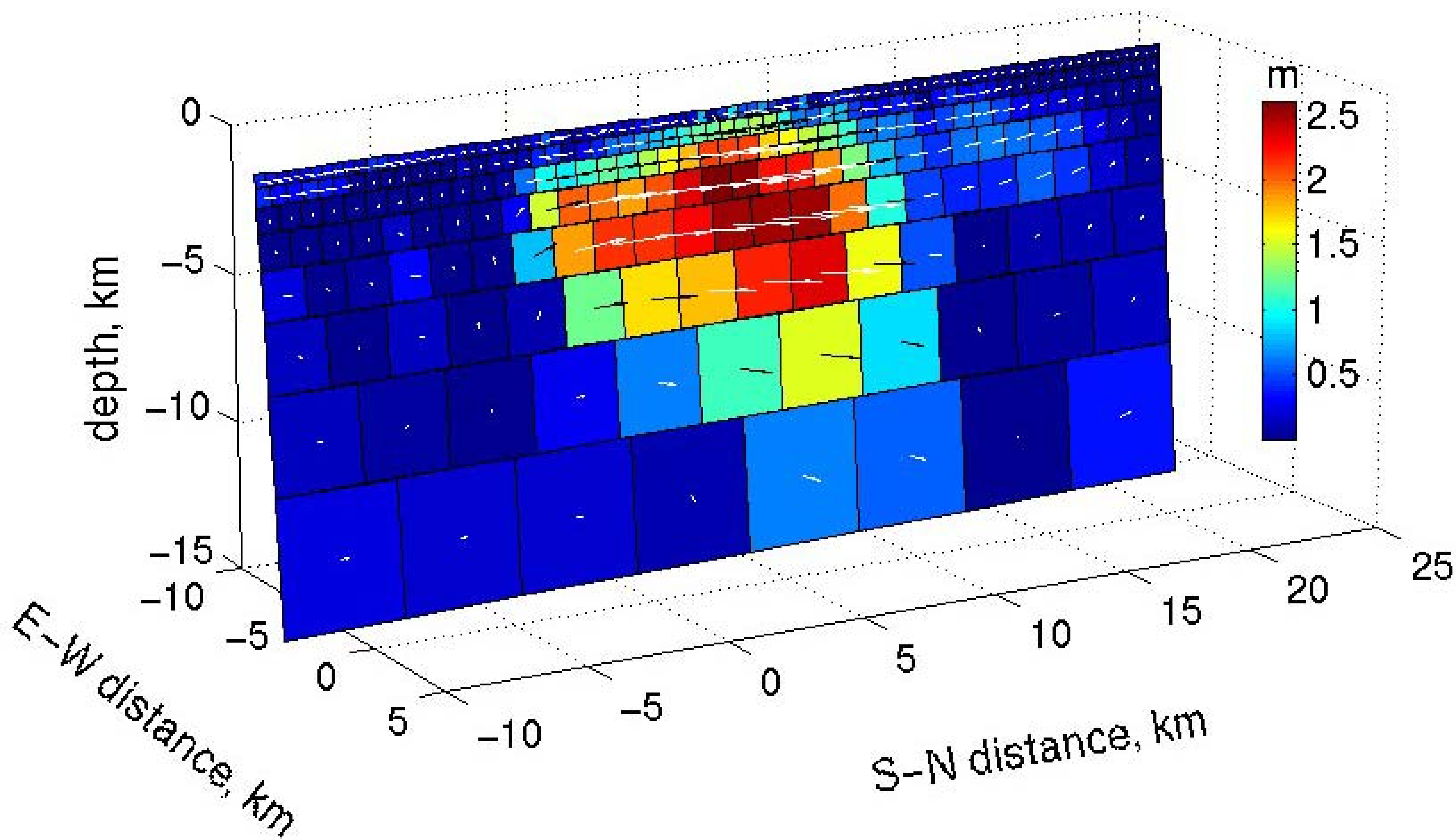

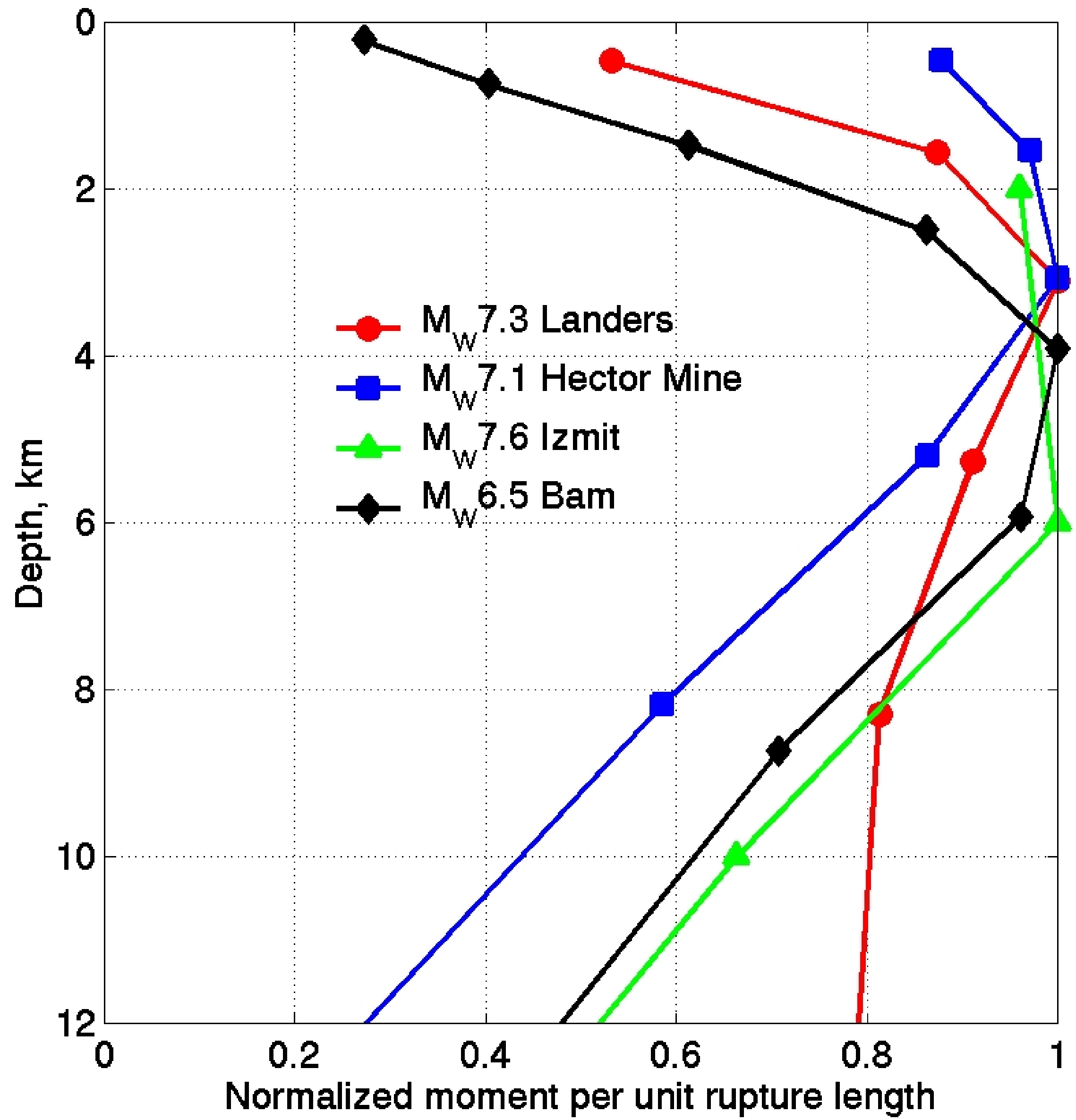

0
2
4
6
8
10
12
Depth, km
0
0.2
0.4
0.6
0.8
1
Normalized moment per unit rupture length
M_W 7.3 Landers
M_W 7.1 Hector Mine
M_W 7.6 Izmit
M_W 6.5 Bam

Kagan, JGR 2004

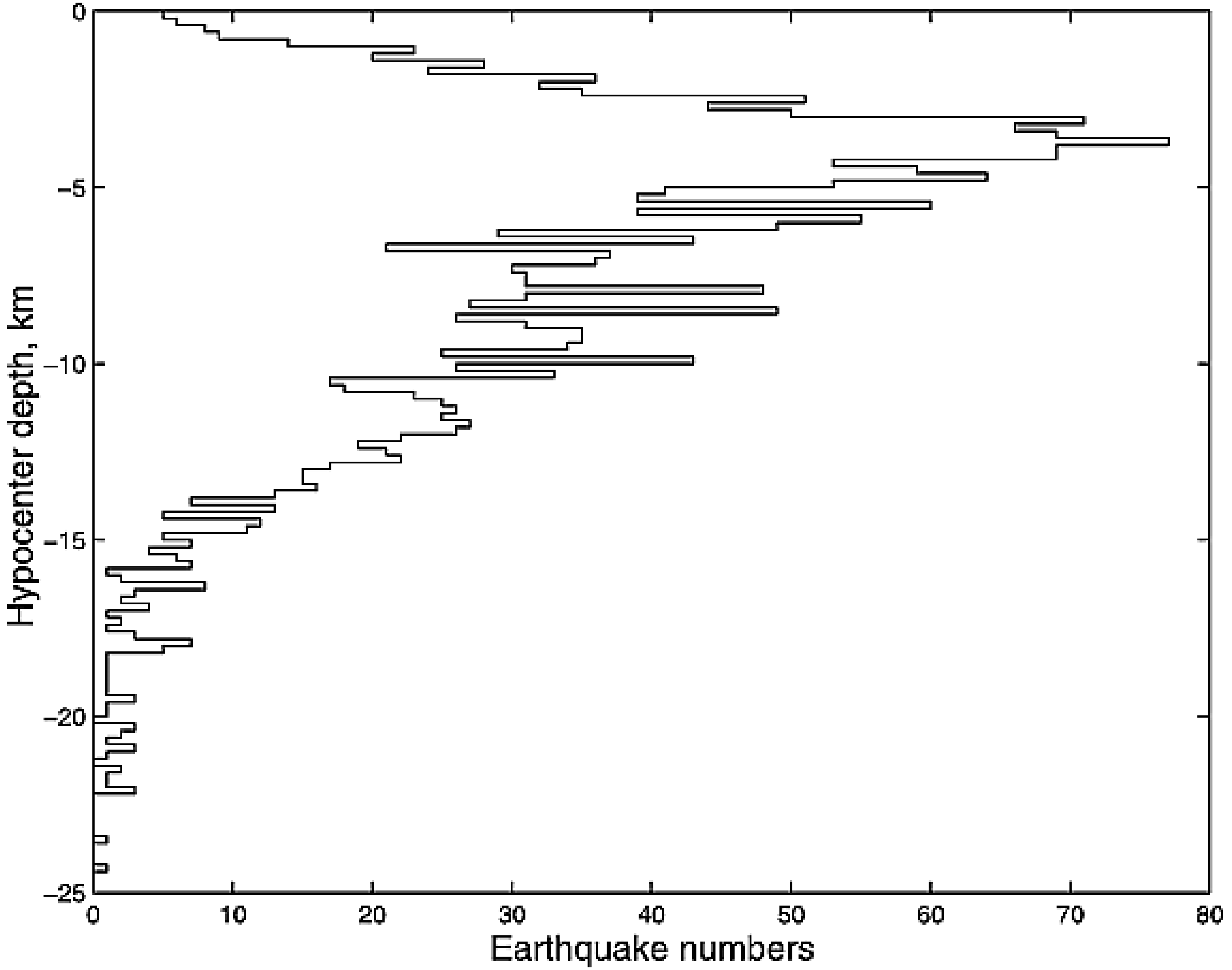

# Proposed mechanisms of post-seismic deformation:

- Afterslip on or below the seismic rupture (Shen et al., 1993; Savage and Svarc, 1997)
- Poro-elastic rebound (Peltzer et al., 1996; 1998; Jonsson et al., 2003)
- Visco-elastic relaxation (Deng et al., 1998; Pollitz et al., 2000; Freed and Burgmann, 2004)
- Combination of mechanisms (Masterlark and Wang, 2002; Fialko, 2004)

# How localized is postseismic deformation in the ductile substrate?

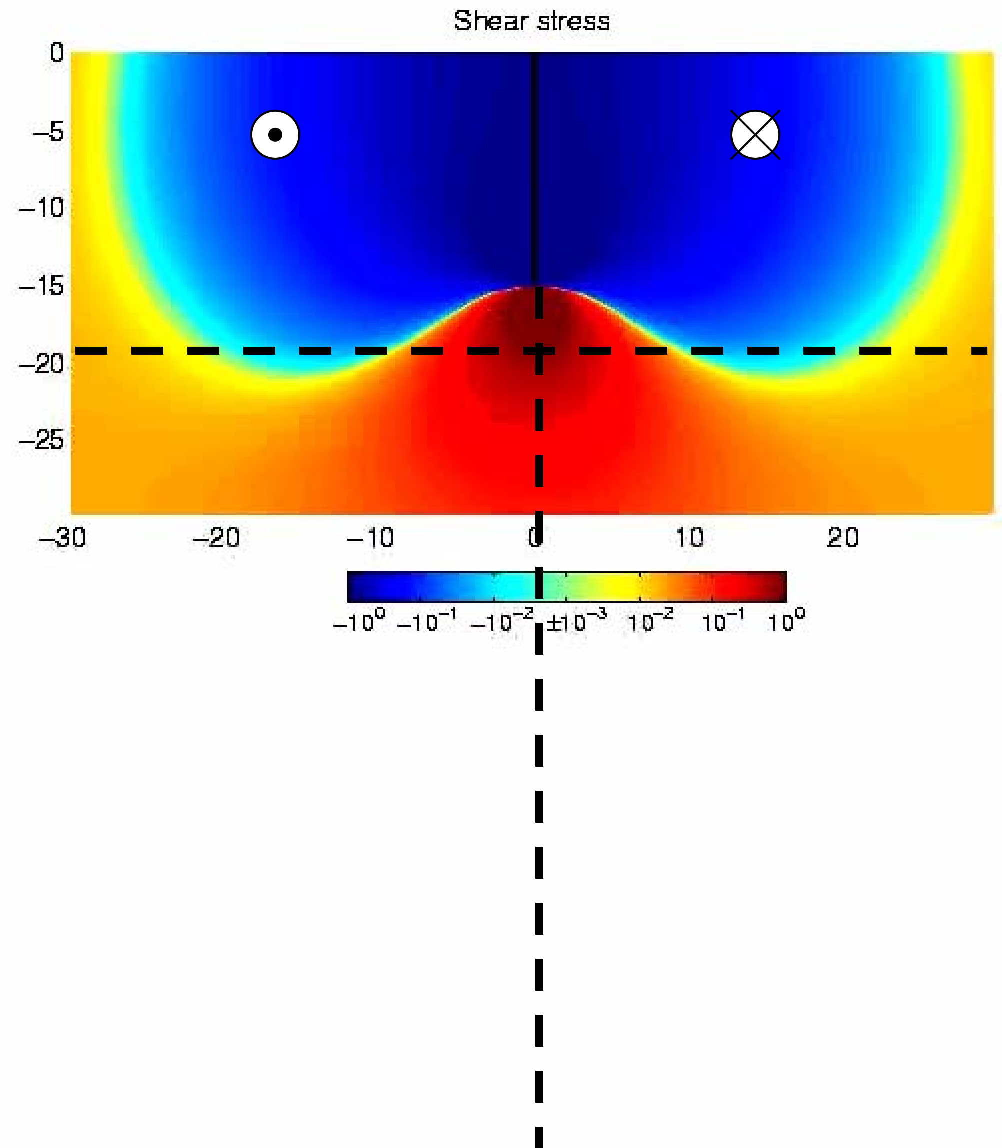
Shear stress
0
−5
−10
−15
−20
−25
−30
−20
−10
0
10
20
$-10^0$ $-10^{-1}$ $-10^{-2}$ $\pm 10^{-3}$ $10^{-2}$ $10^{-1}$ $10^0$

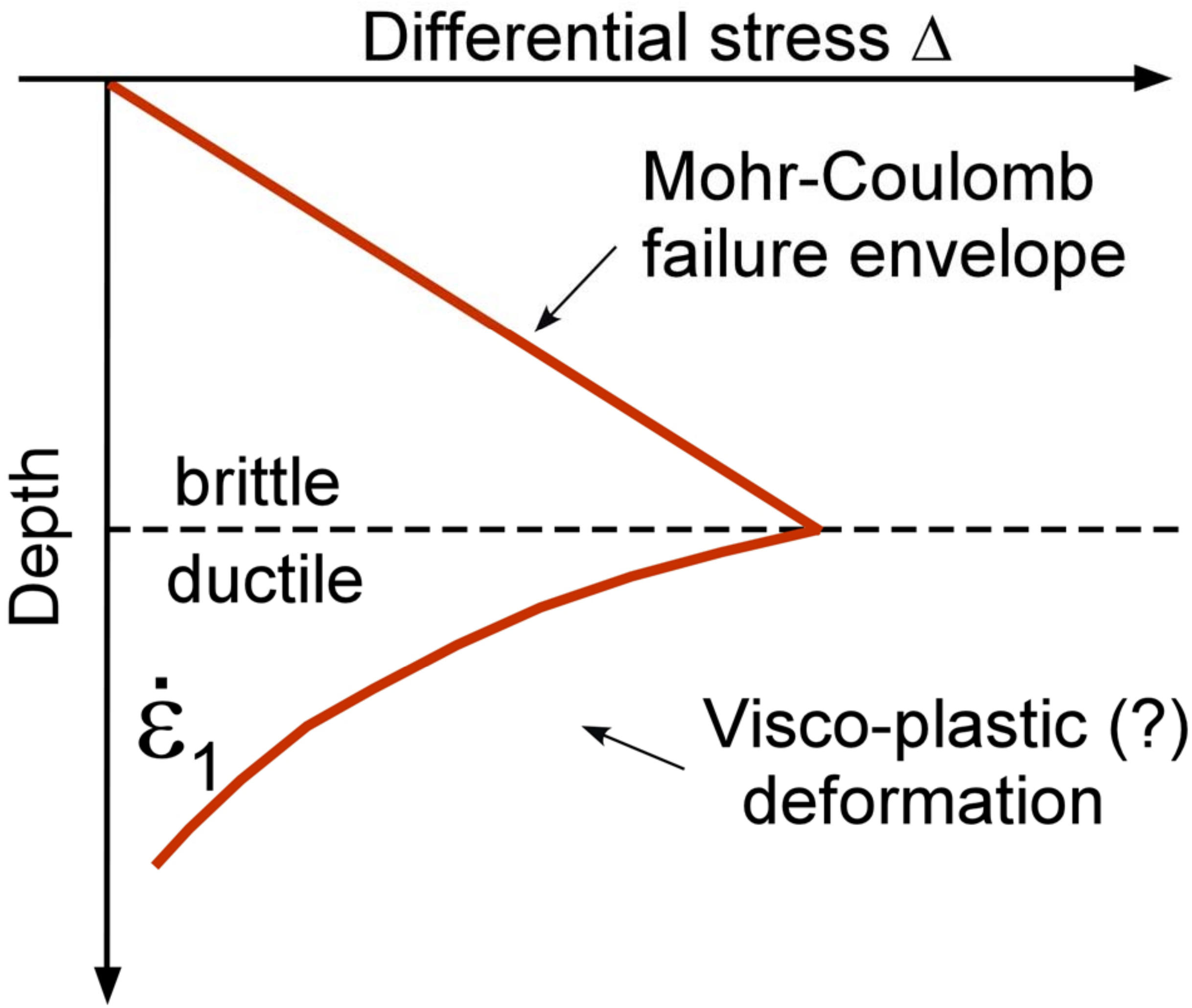
Differential stress Δ
Mohr-Coulomb
failure envelope
brittle
ductile
Depth
$\dot{\varepsilon}_1$
Visco-plastic (?)
deformation

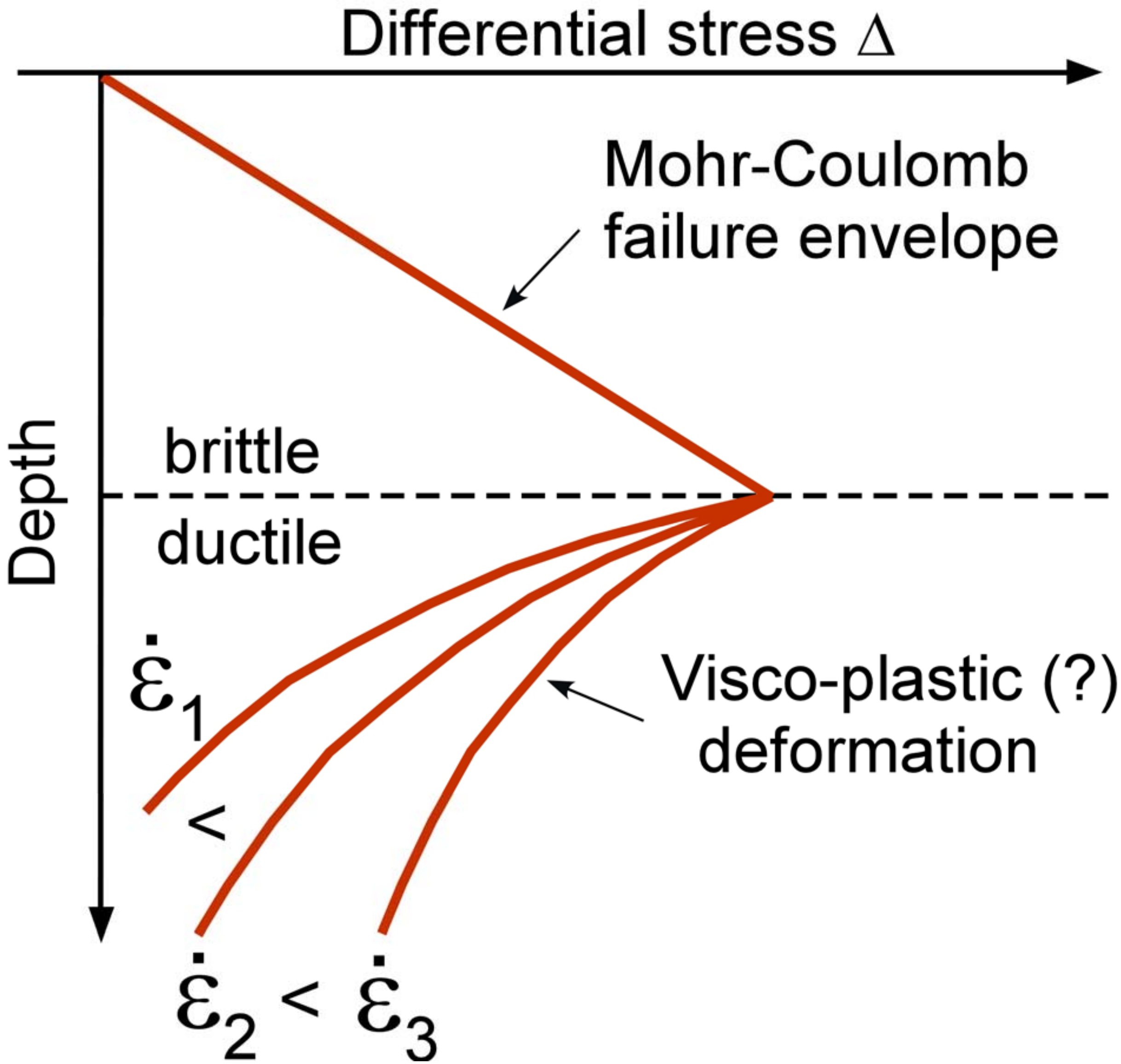
Differential stress Δ
Mohr-Coulomb
failure envelope
Depth
brittle
ductile
$\dot{\varepsilon}_1$
<
$\dot{\varepsilon}_2$ < $\dot{\varepsilon}_3$
Visco-plastic (?)
deformation

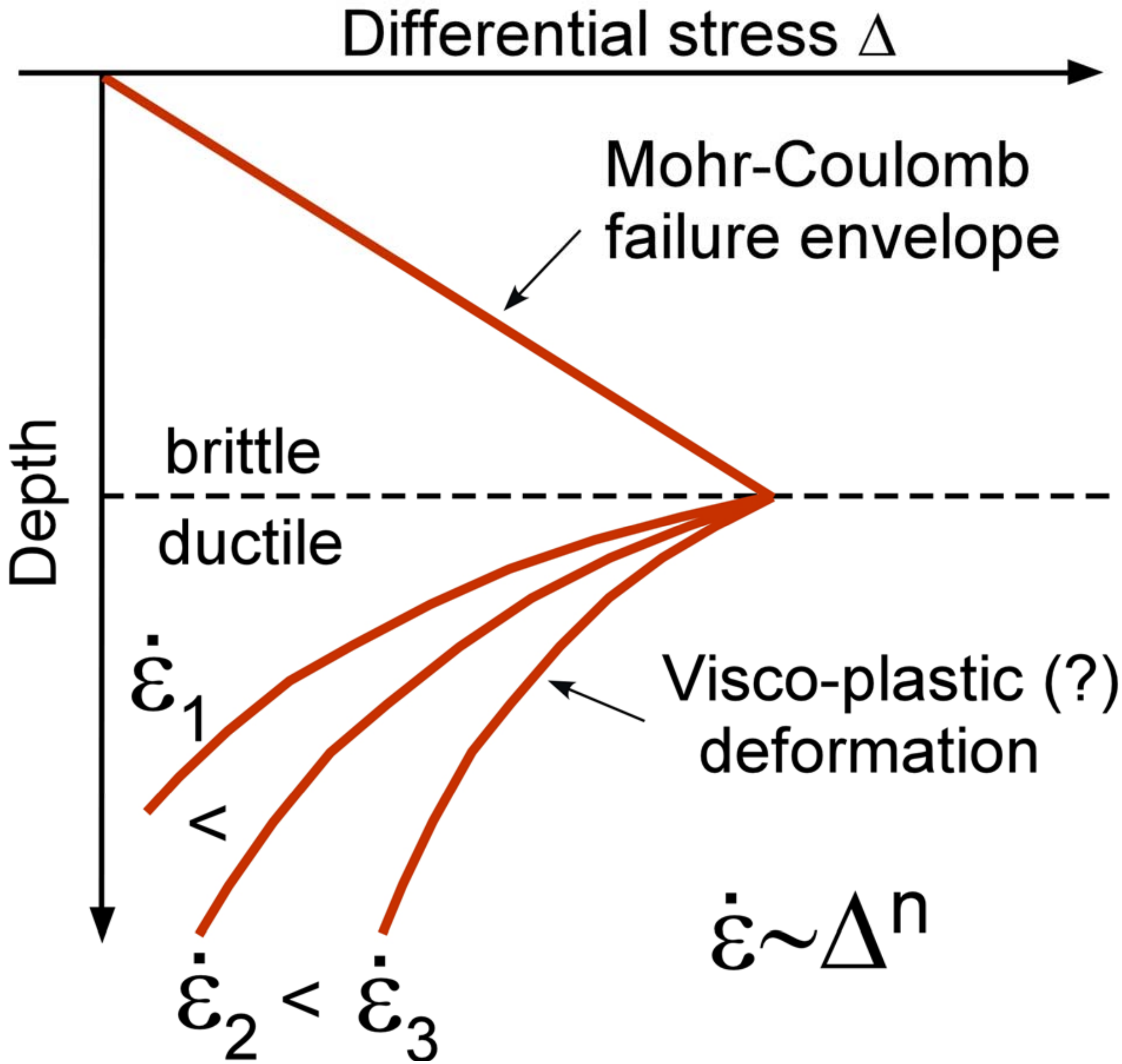
Differential stress Δ
Mohr-Coulomb
failure envelope
Depth
brittle
ductile
$\dot{\varepsilon}_1$
<
$\dot{\varepsilon}_2$ < $\dot{\varepsilon}_3$
Visco-plastic (?)
deformation
$\dot{\varepsilon} \sim \Delta^n$

$\sigma_{ij}^{0}$ initial (interseismic) stress state

$\sigma_1^0, \sigma_2^0, \sigma_3^0$ principal stresses

$$\sigma_1^0 - \sigma_3^0 = C$$

$$(\sigma_1^0 - \sigma_3^0)^2 + (\sigma_2^0 - \sigma_3^0)^2 +$$

$$(\sigma_1^0 - \sigma_2^0)^2 = S^2$$

$$\sigma_{ij}^{0} + \sigma_{ij}^{c} \rightarrow \sigma_{ij}^{*} + \sigma_{ij}^{r}$$

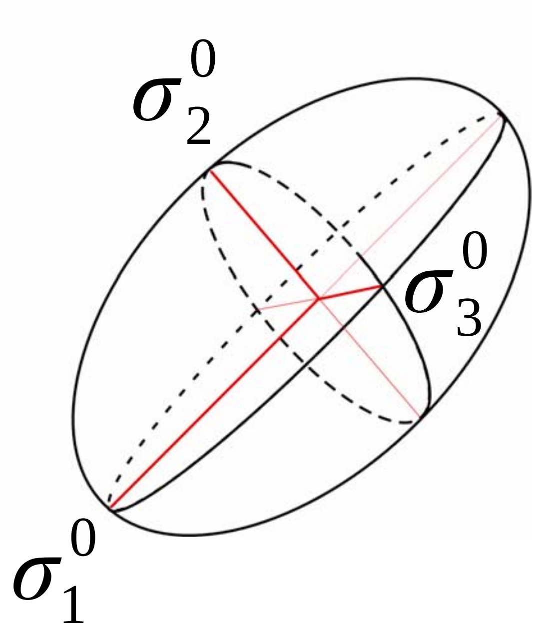


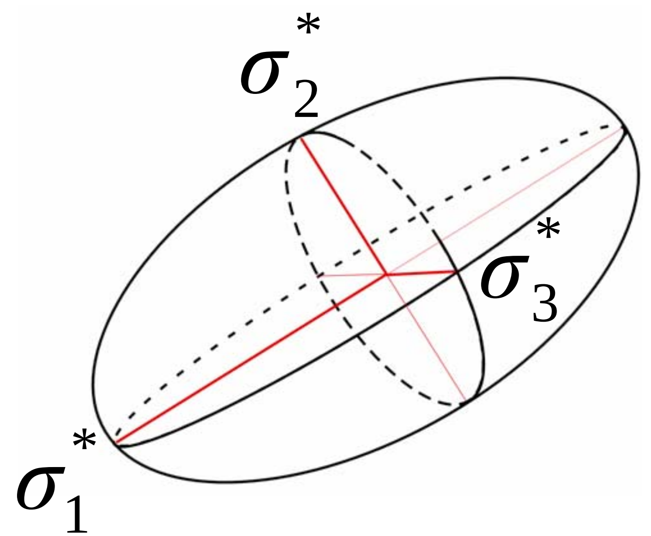

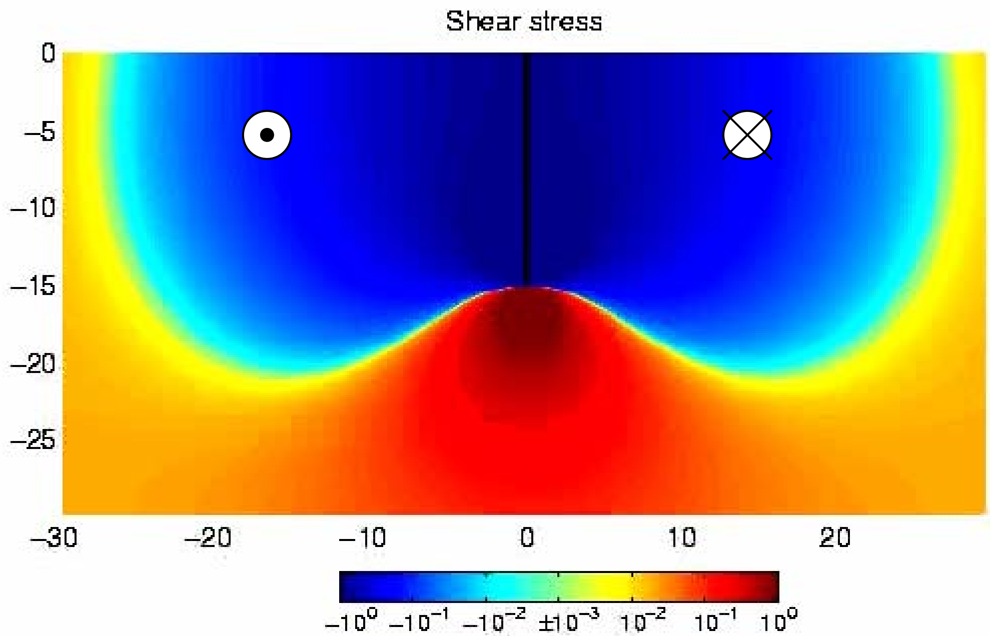
Shear stress
0
−5
−10
−15
−20
−25
−30
−20
−10
0
10
20
$-10^0$ $-10^{-1}$ $-10^{-2}$ $\pm10^{-3}$ $10^{-2}$ $10^{-1}$ $10^0$

# 3-D models: Vertical displacements

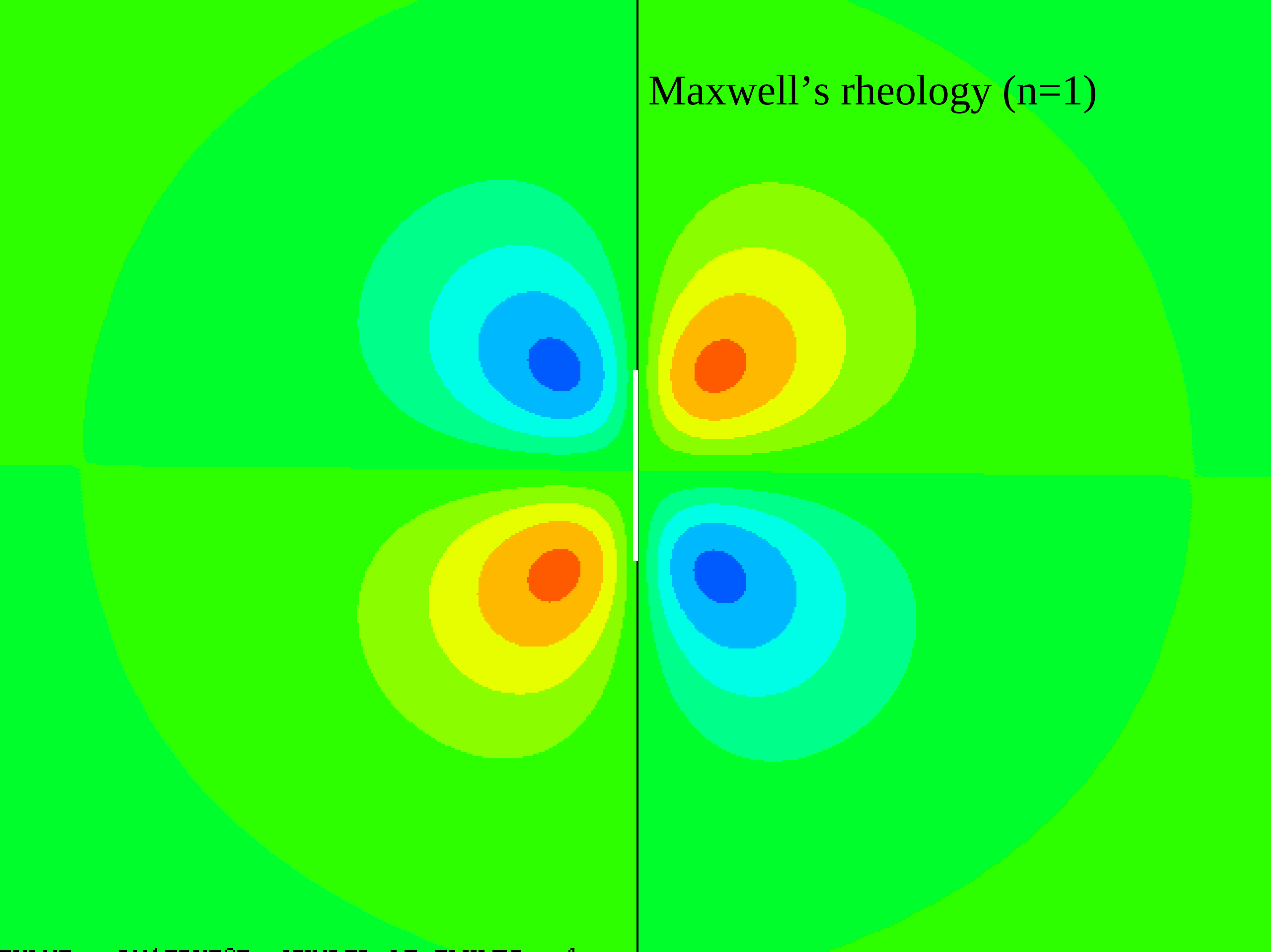
Maxwell’s rheology (n=1)

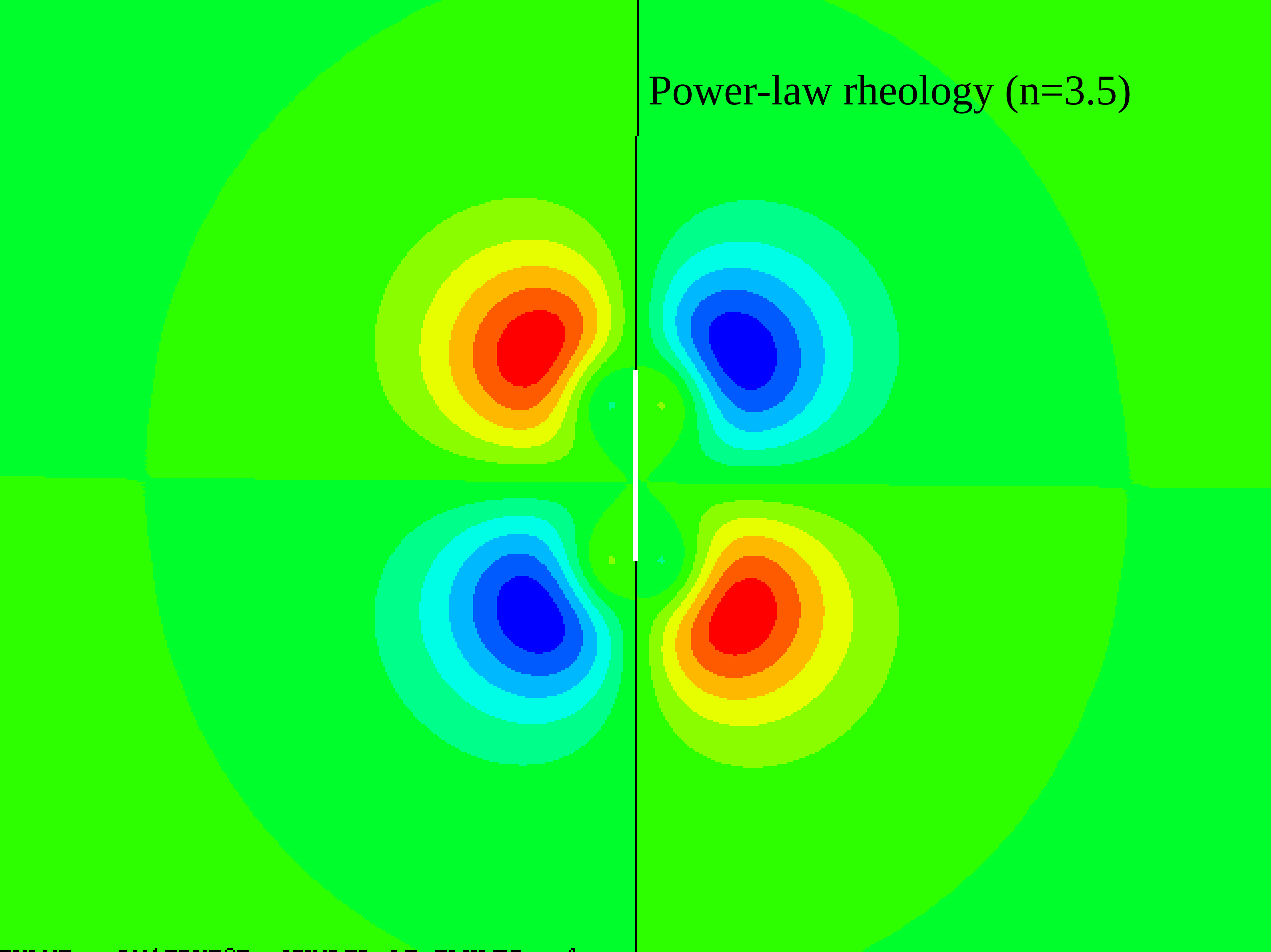
Power-law rheology (n=3.5)

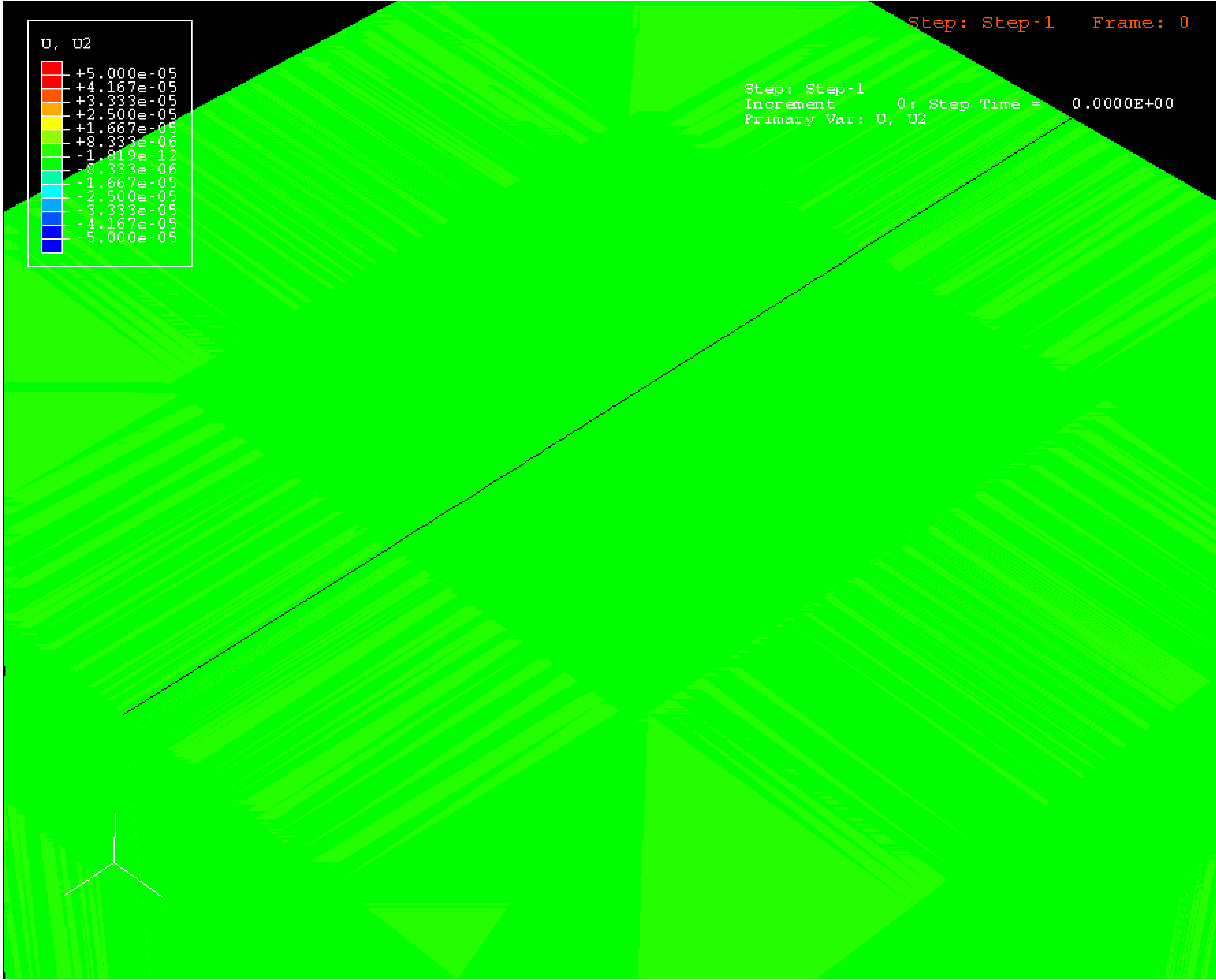
U, U2
+5.000e-05
+4.167e-05
+3.333e-05
+2.500e-05
+1.667e-05
+8.333e-06
-1.819e-12
-8.333e-06
-1.667e-05
-2.500e-05
-3.333e-05
-4.167e-05
-5.000e-05
Step: Step-1 Frame: 0
Step: Step-1
Increment 0: Step Time = 0.0000E+00
Primary Var: U, U2

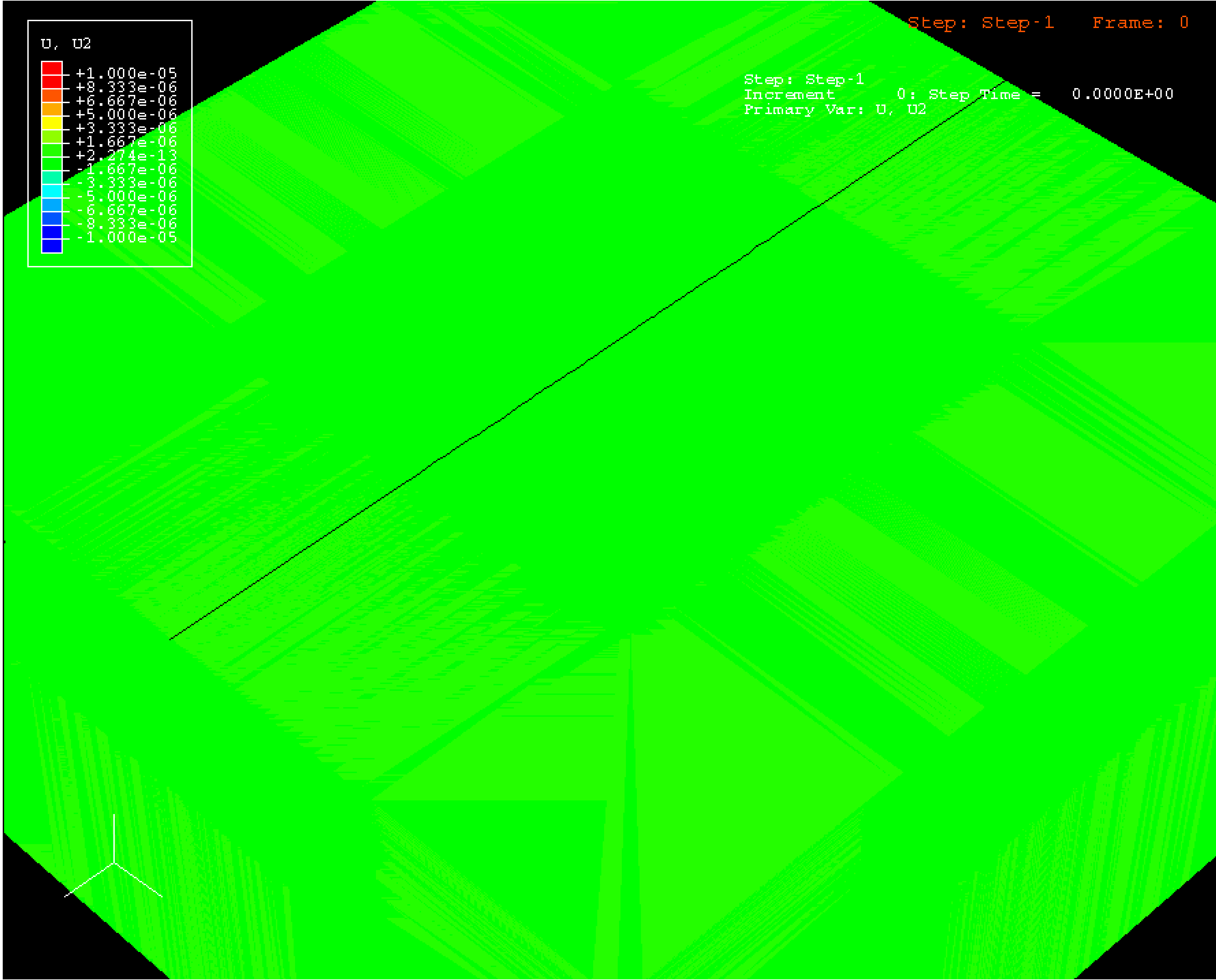
U, U2
+1.000e-05
+8.333e-06
+6.667e-06
+5.000e-06
+3.333e-06
+1.667e-06
+2.274e-13
-1.667e-06
-3.333e-06
-5.000e-06
-6.667e-06
-8.333e-06
-1.000e-05
Step: Step-1 Frame: 0
Step: Step-1
Increment 0: Step Time = 0.0000E+00
Primary Var: U, U2

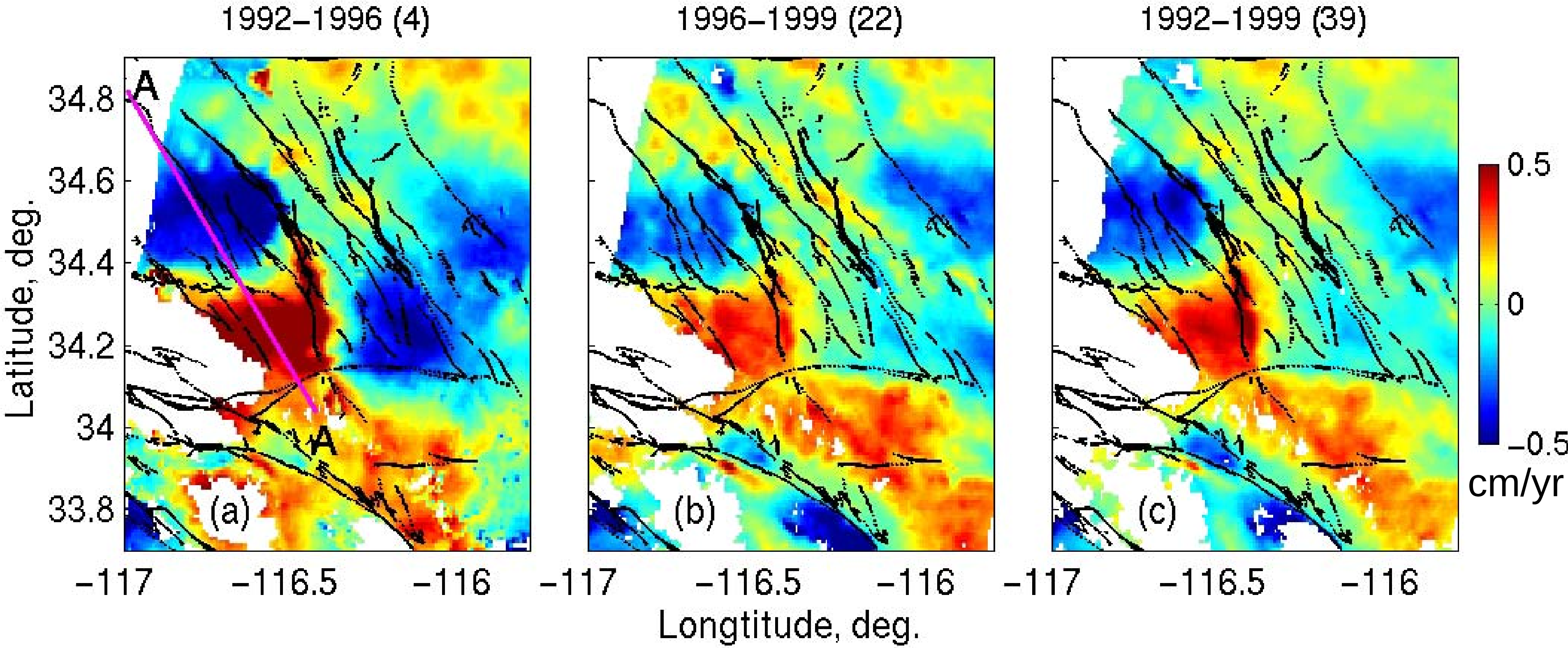

1992–1996 (4)
1996–1999 (22)
1992–1999 (39)
Latitude, deg.
34.8
34.6
34.4
34.2
34
33.8
A
A
(a)
(b)
(c)
0.5
0
−0.5
cm/yr
−117
−116.5
−116
Longtitude, deg.

# Horizontal displacements alone: are they a good discriminant?

Pollitz, 1997; Hearn, 2003; Fialko, 2004

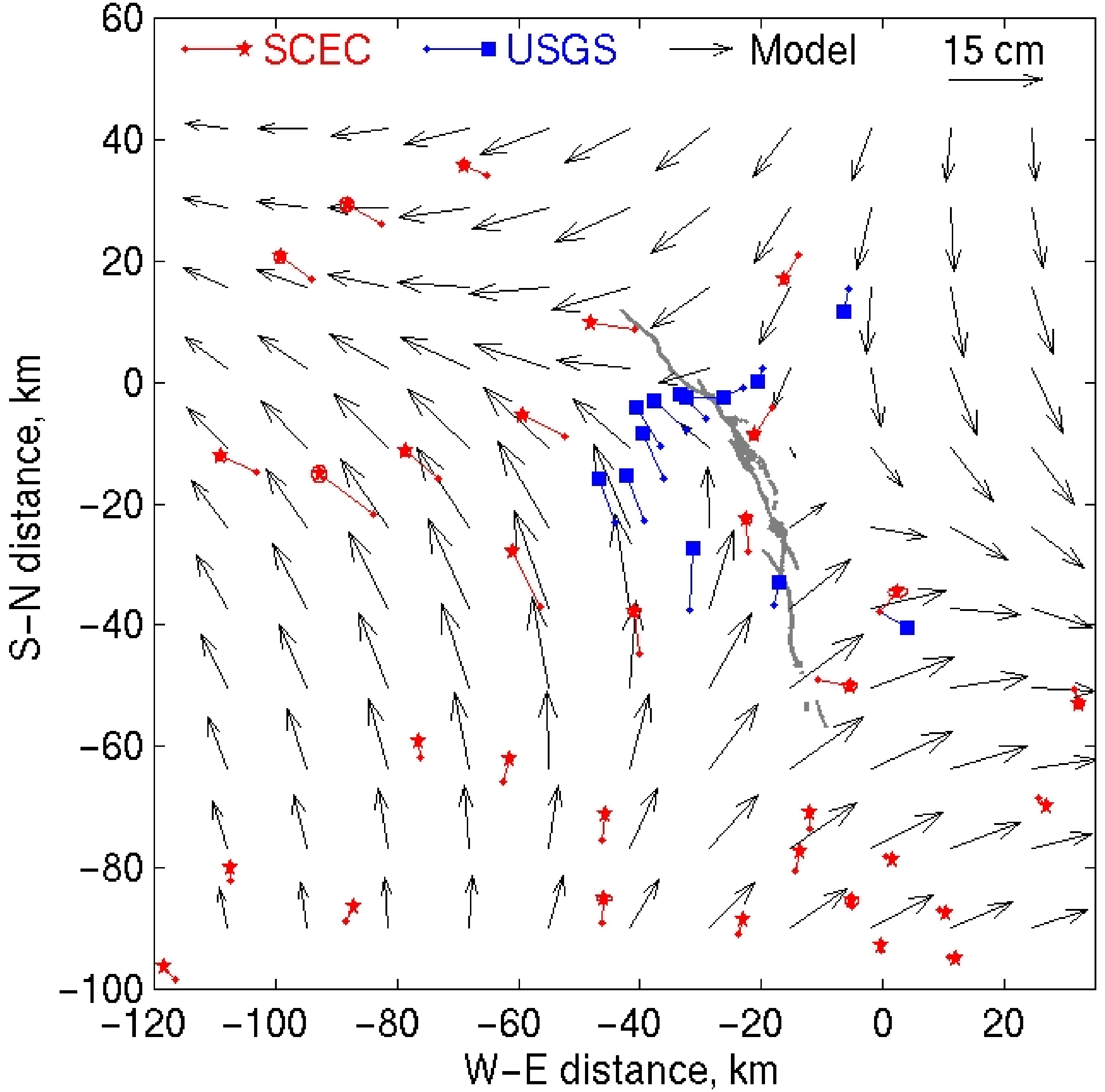

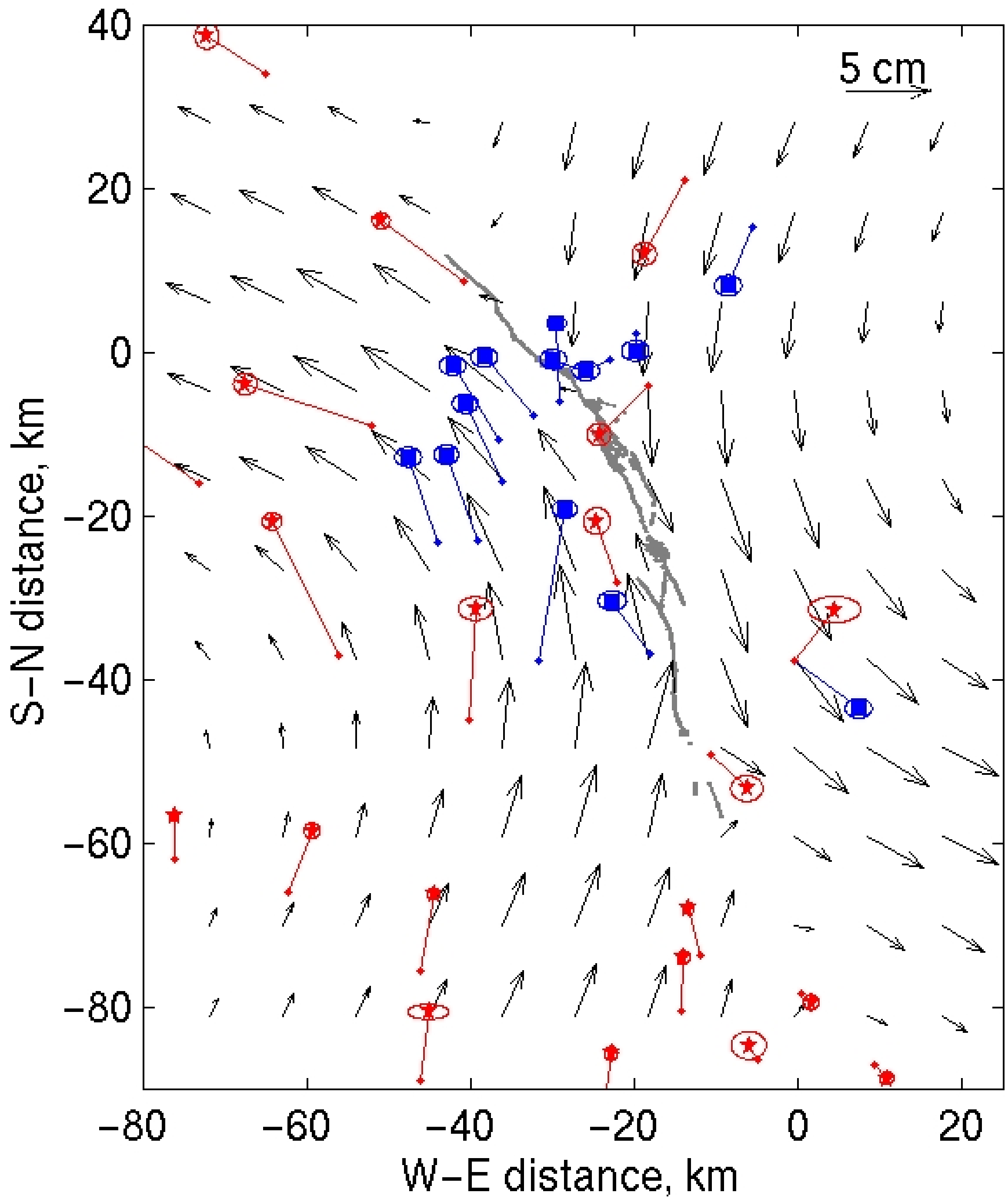

5 cm
S–N distance, km
W–E distance, km
40
20
0
−20
−40
−60
−80
−80
−60
−40
−20
0
20

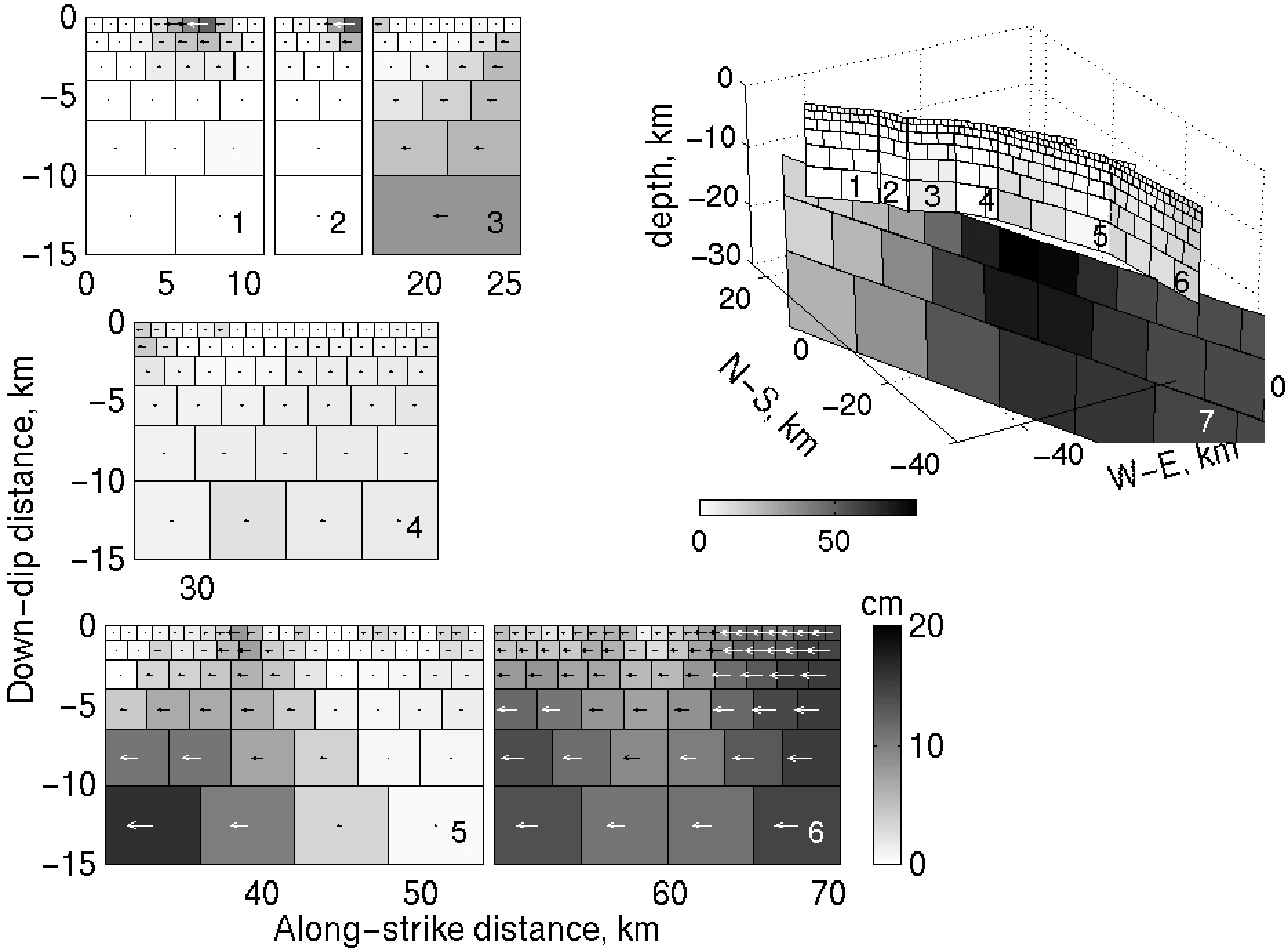

Down-dip distance, km
Along-strike distance, km
depth, km
N-S, km
W-E, km
cm
1
2
3
4
5
6
7

# Time dependence and “permanent” postseismic deformation

Freed and Burgmann, Nature 2004

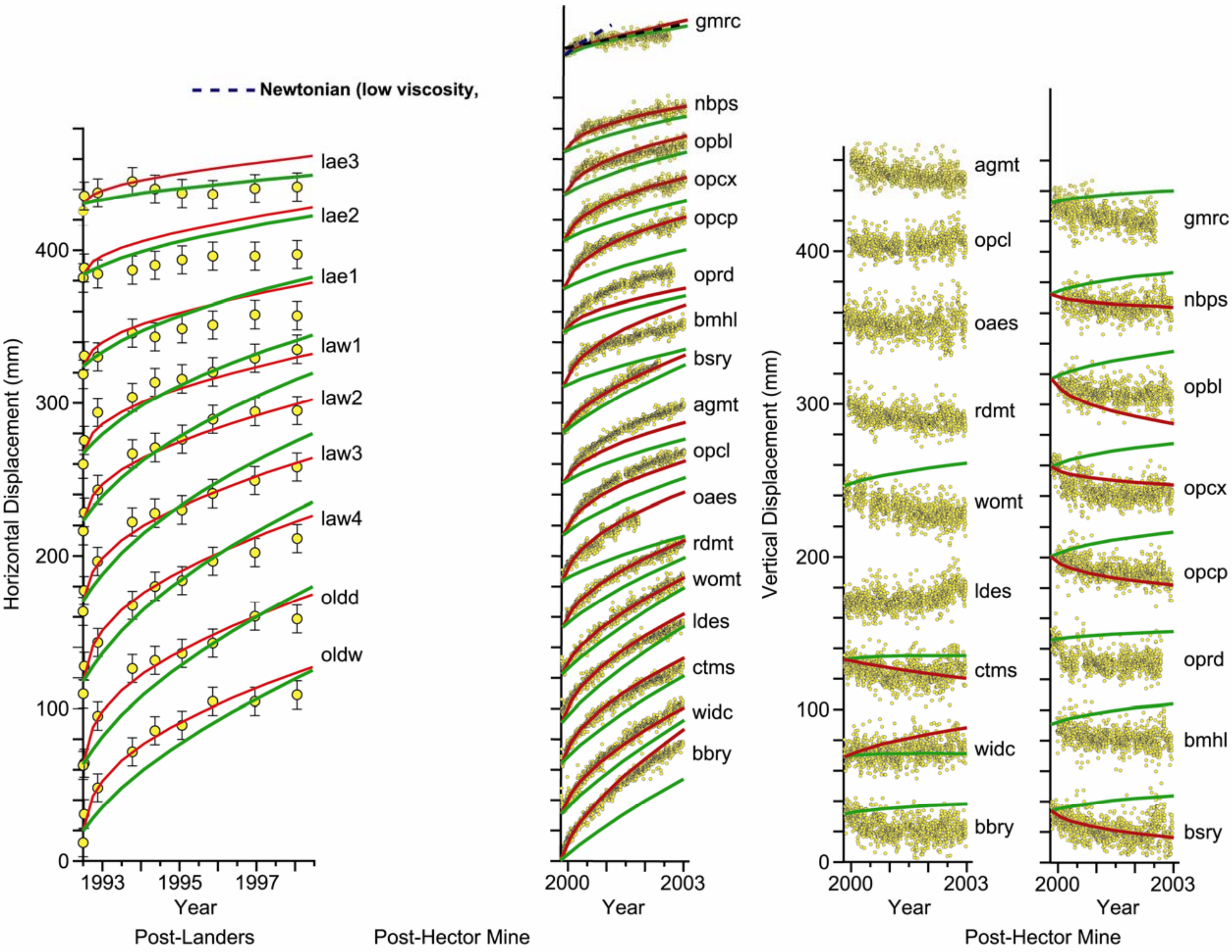

Savage et al., JGR 2003; Fialko, JGR 2004

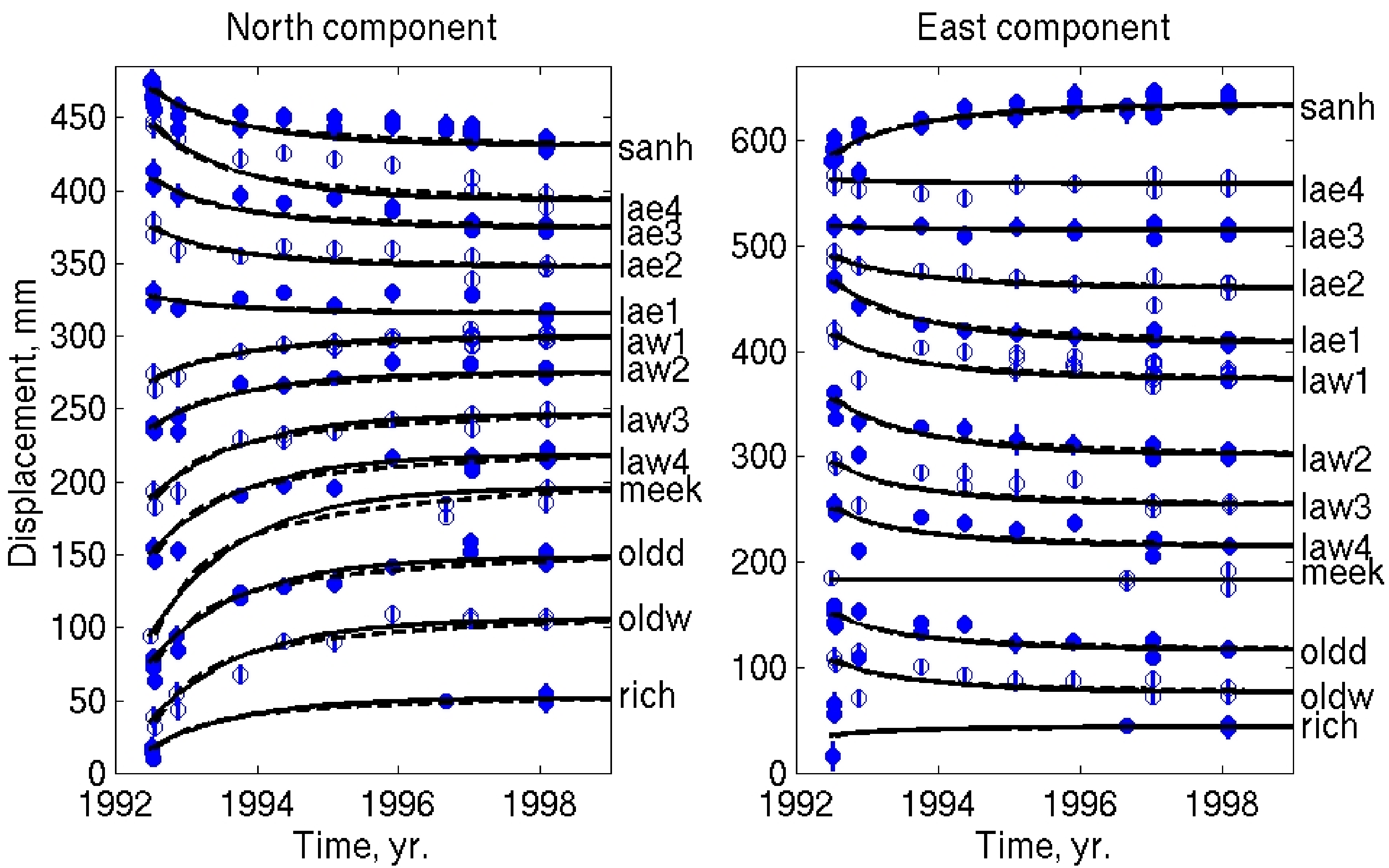

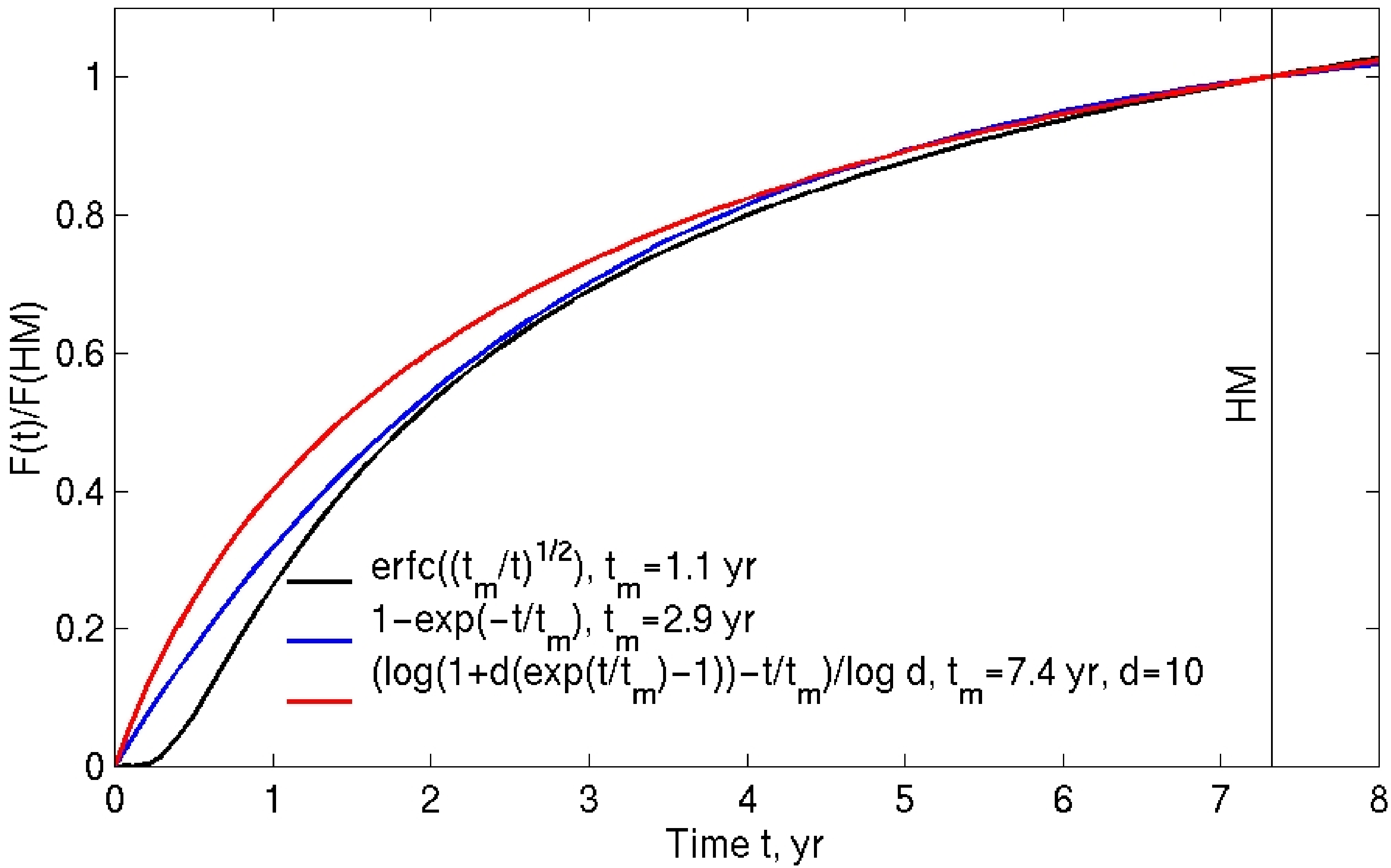

F(t)/F(HM)
Time t, yr
HM
0
0.2
0.4
0.6
0.8
1
0
1
2
3
4
5
6
7
8
erfc((t_m/t)^{1/2}), t_m=1.1 yr
1−exp(−t/t_m), t_m=2.9 yr
(log(1+d(exp(t/t_m)−1))−t/t_m)/log d, t_m=7.4 yr, d=10

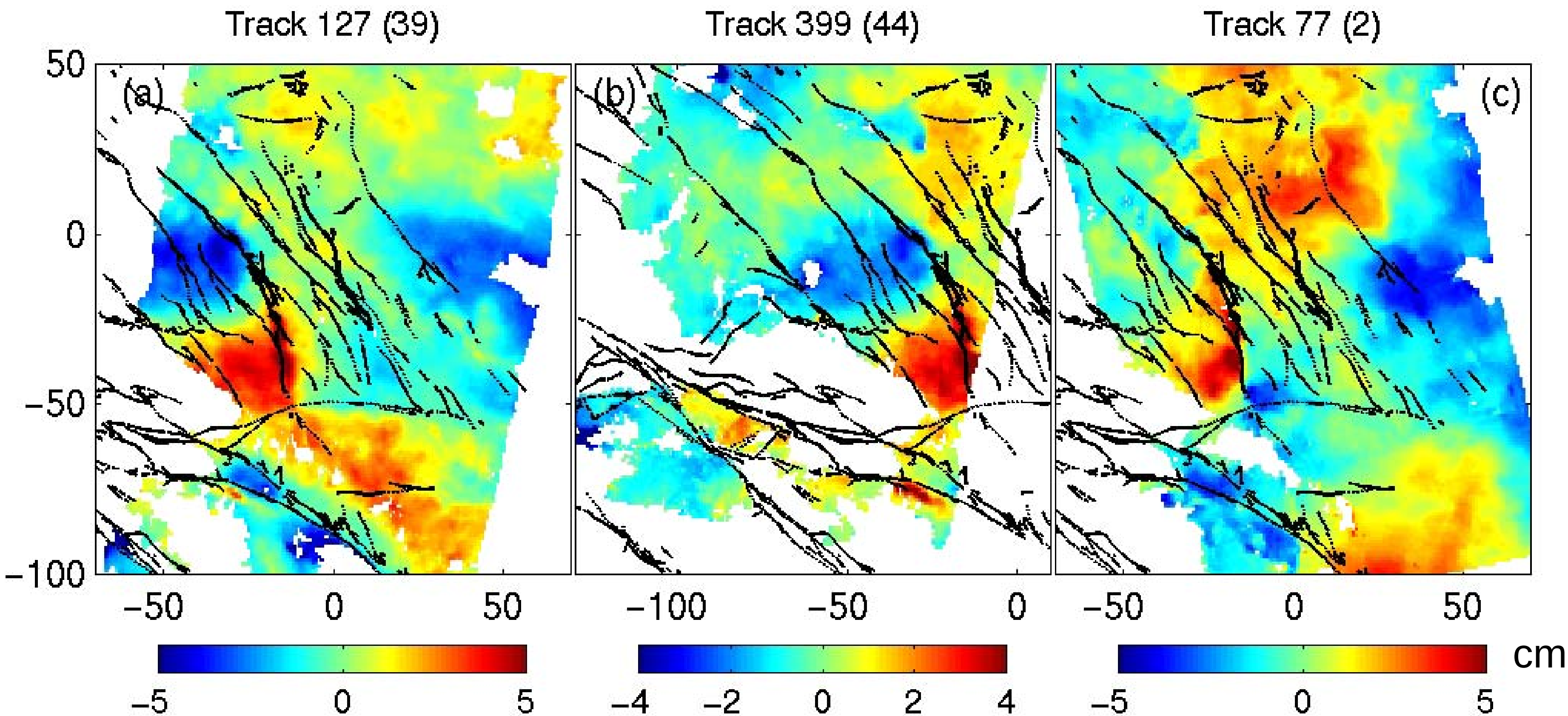

Track 127 (39)
Track 399 (44)
Track 77 (2)
(a)
(b)
(c)
50
0
−50
−100
−50
0
50
−100
−50
0
−50
0
50
−5
0
5
−4
−2
0
2
4
−5
0
5
cm

# Visco-elastic relaxation

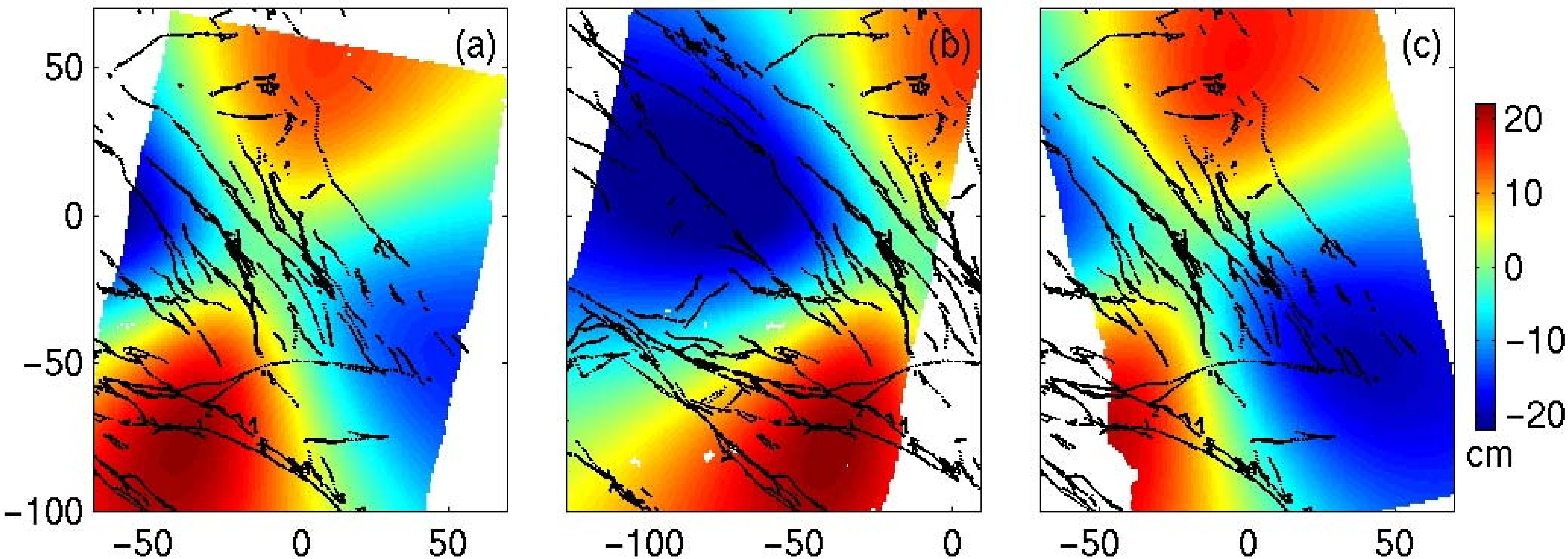

# Long-term deformation (multiple faults, multiple eq cycles) :

- Long-term vs short-term rheology
- Large strains
  - Elastic
  - Inelastic
- Treatment of plasticity (localization)
- “Pre-stress” -> ambient stress
- Forcing (Paleoseismicity? Spontaneous rupture nucleation?)

# V 6.6 (as of May 2006)

ABAQUS

### ABAQUS/AMS

- ABAQUS/AMS (Automatic Multi-level Substructuring) is an add-on product that provides significant performance advantages for natural frequency extraction simulations, especially for large models and the extraction of large numbers of eigenmodes. Benchmarks indicate that the use of ABAQUS/AMS can result in 10–25 times faster turnaround times compared to the default Lanczos method.

### Supported Platforms

ABAQUS Version 6.6-1 supports the platforms listed in the table below. As usual, ABAQUS probably will run on later operating systems, but not on earlier ones.

| Platform/Processor | Operating System (Tier 1 test configuration) | CAE | Viewer | Analysis Products |
|---|---|---|---|---|
| Windows/x86-32 | Windows XP | Yes | Yes | Yes |
| Linux/x86-32 | SuSE Linux 8.2 | Yes | Yes | Yes |
| HP-UX/Itanium | HP-UX B.11.22 | No | No | Yes |
| Linux/Itanium | SuSE Linux Enterprise Server 9.0 | No | No | Yes |
| Linux/x86-64 | SuSE 9.0 | Yes | Yes | Yes |

ABAQUS Version 6.6 will be released on additional platforms in future maintenance releases. Please go to `www.abaqus.com`→**Support & Services→Technical Support→Systems Information→ ABAQUS Version 6.6 Supported Platforms and Products** for a complete set of supported platform, chipset, and operating system details.

## Key Features of Version 6.6-1

Some of the key features of Version 6.6-1 follow:

### Adaptive remeshing

- The quality of ABAQUS/Standard simulation results can be improved for situations when you are unsure how refined the mesh needs to be to reach a desired level of accuracy. This capability utilizes the close interaction of ABAQUS/Standard and ABAQUS/CAE to arrive iteratively at a mesh that improves solution accuracy for a wide range of applications.

### Visualization enhancements

- Numerous enhancements are introduced to improve postprocessing capabilities, particularly for complex nonlinear simulations.
  - Animation functionality is extended in several ways, including synchronizing animations and overlay of simulation results with imported "movies," such as an experimental test.
  - *X–Y* plots can now be animated, including synchronization with other animated viewports.
  - Plot states are now available. Plot states enable multiple plot types and options to be invoked in a single viewport with a streamlined and unified user interface.

### Fracture and failure modeling enhancements

- A damage model for fiber-reinforced composite materials is available in ABAQUS/Standard and supported in ABAQUS/CAE, complementing the existing cohesive element capabilities and optional VCCT technology already available in ABAQUS.
- Cohesive elements can be used in import simulations to transfer analysis results between ABAQUS/Standard and ABAQUS/Explicit, as well as between two ABAQUS/Standard simulations.
- Connector damage and failure effects can now be defined in ABAQUS/Standard (as already available in ABAQUS/Explicit). This provides for realistic modeling of damage and failure in discrete connections, such as spot welds and rivets.
- The Johnson-Cook criterion for damage initiation in ductile metals is now available within the general framework of progressive damage and failure in ABAQUS/Explicit.
- Material damage initiation criteria and damage evolution can now be defined in ABAQUS/CAE.

### Improved performance of ABAQUS analysis products

- Both serial and parallel performance is improved significantly in ABAQUS/Explicit. For certain classes of large models ABAQUS/Explicit can now effectively use up to 16–32 CPUs.
- A distributed memory parallel (DMP) direct sparse solver is introduced in ABAQUS/Standard. With this new functionality, it is now possible for large classes of problems in both ABAQUS/Standard and ABAQUS/Explicit to run on popular distributed memory cluster systems.
- The quasi-Newton solution technique in ABAQUS/Standard is enhanced to provide substantial performance gains for certain types of nonlinear static and dynamic simulations.
- Support for the parallel execution of the element operations in ABAQUS/Standard is extended to include more procedure types.

### Contact enhancements

- Several enhancements are implemented to improve the convergence and the accuracy of simulations involving contact in ABAQUS/Standard.
  - A penalty method for enforcing contact conditions is available, providing for more efficient convergence behavior in many cases.
  - A true surface-to-surface formulation for finite-sliding contact is available, providing better stress accuracy, along with the ability to account easily for surface thicknesses in contact (such as shell or membrane thickness).
  - A new approach is available to deal with severe discontinuity iterations (SDIs), those iterations in which the contact state at one or more points changes during the course of the iteration. Severe discontinuities can be converted automatically to force residuals, potentially improving convergence behavior for simulations involving contact "chattering" and those in which a large number of SDIs previously have been required to settle the contact conditions.
- Contact capabilities are also enhanced in ABAQUS/Explicit.
  - The edge-to-edge feature of the general contact capability is now parallelized, enabling more effective use of multiple CPUs for parallel execution and for reducing overall turnaround time.
  - Analytical rigid surfaces can now be used in conjunction with general contact.

### Model preprocessing enhancements in ABAQUS/CAE

- The Sketch module contains many enhancements to the sketch creation and editing tools, including the implementation of a constraint manager, which provides for the specification of parametric relationships between geometric entities.
- Several previous restrictions associated with virtual topology are eliminated. As a result, the full suite of geometric and mesh creation operations can be applied to parts that include virtual topology.
- The swept meshing technique is generalized to extend its applicability to part geometries and topologies that previously could be meshed only with tetrahedral elements or through the extensive use of partitions.

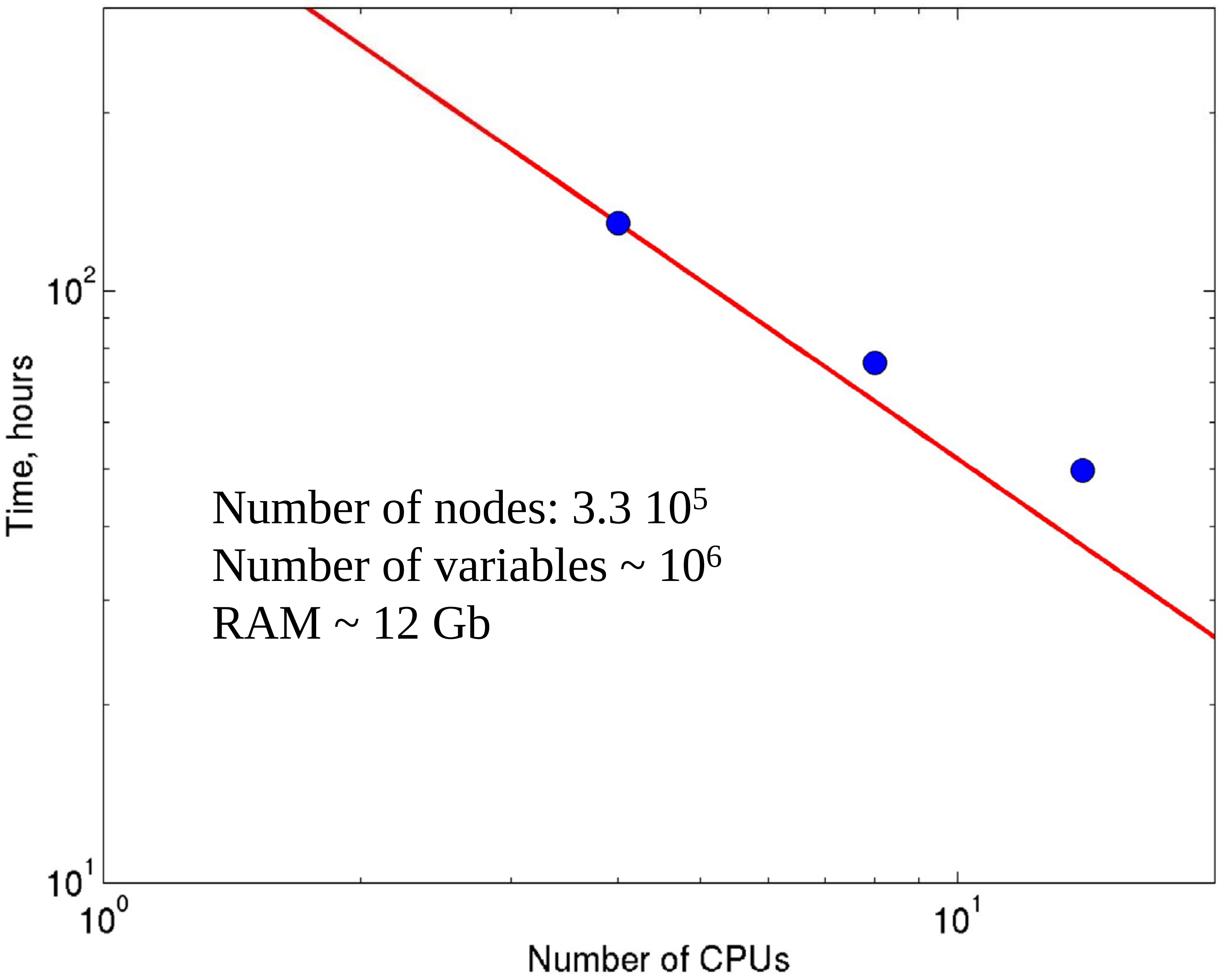

Number of nodes: 3.3 10^5
Number of variables ~ 10^6
RAM ~ 12 Gb
Time, hours
Number of CPUs
10^2
10^1
10^0
10^1

# Post-Hector Mine deformation

Pollitz et al., Science 2001

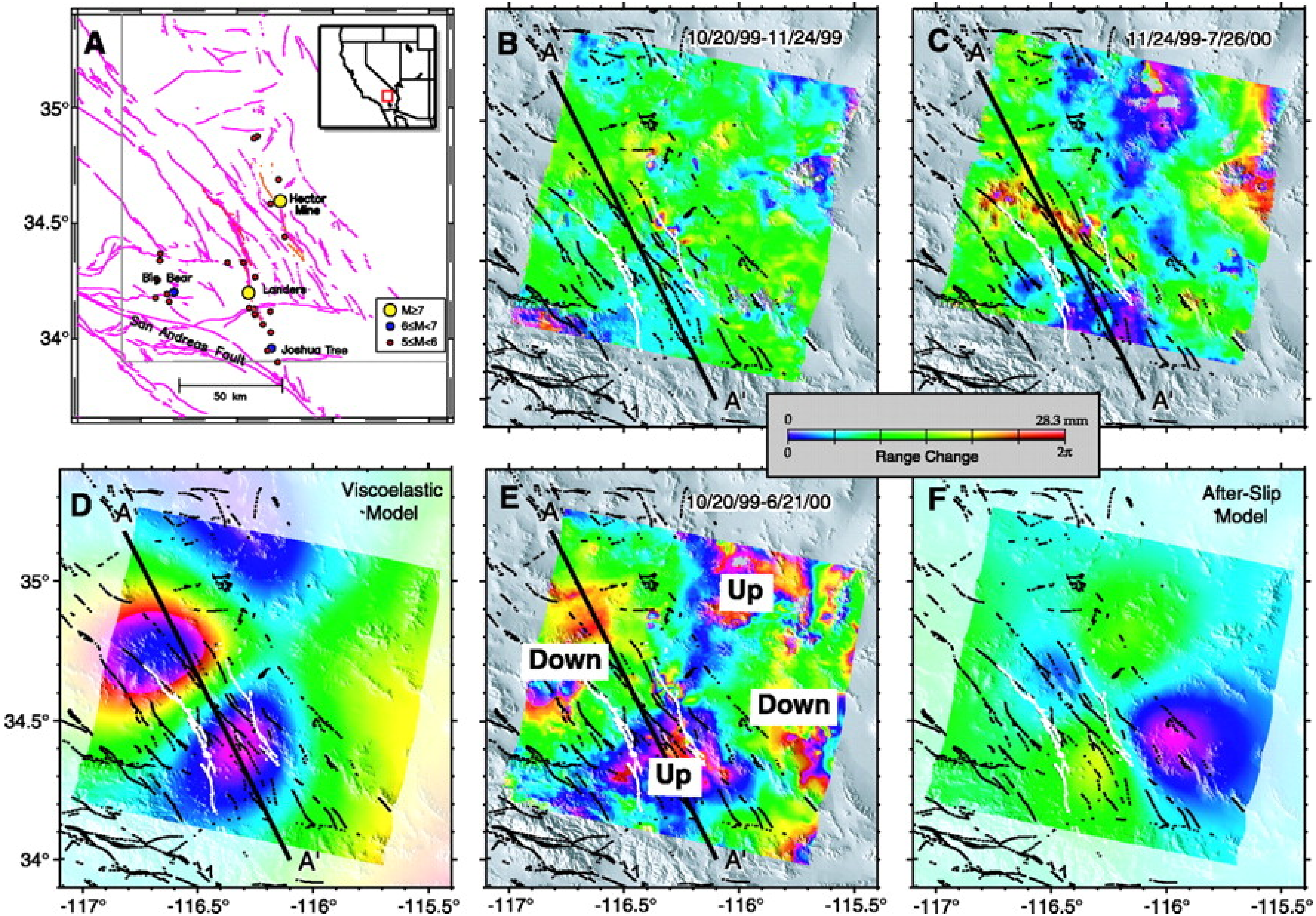

ted
al.,

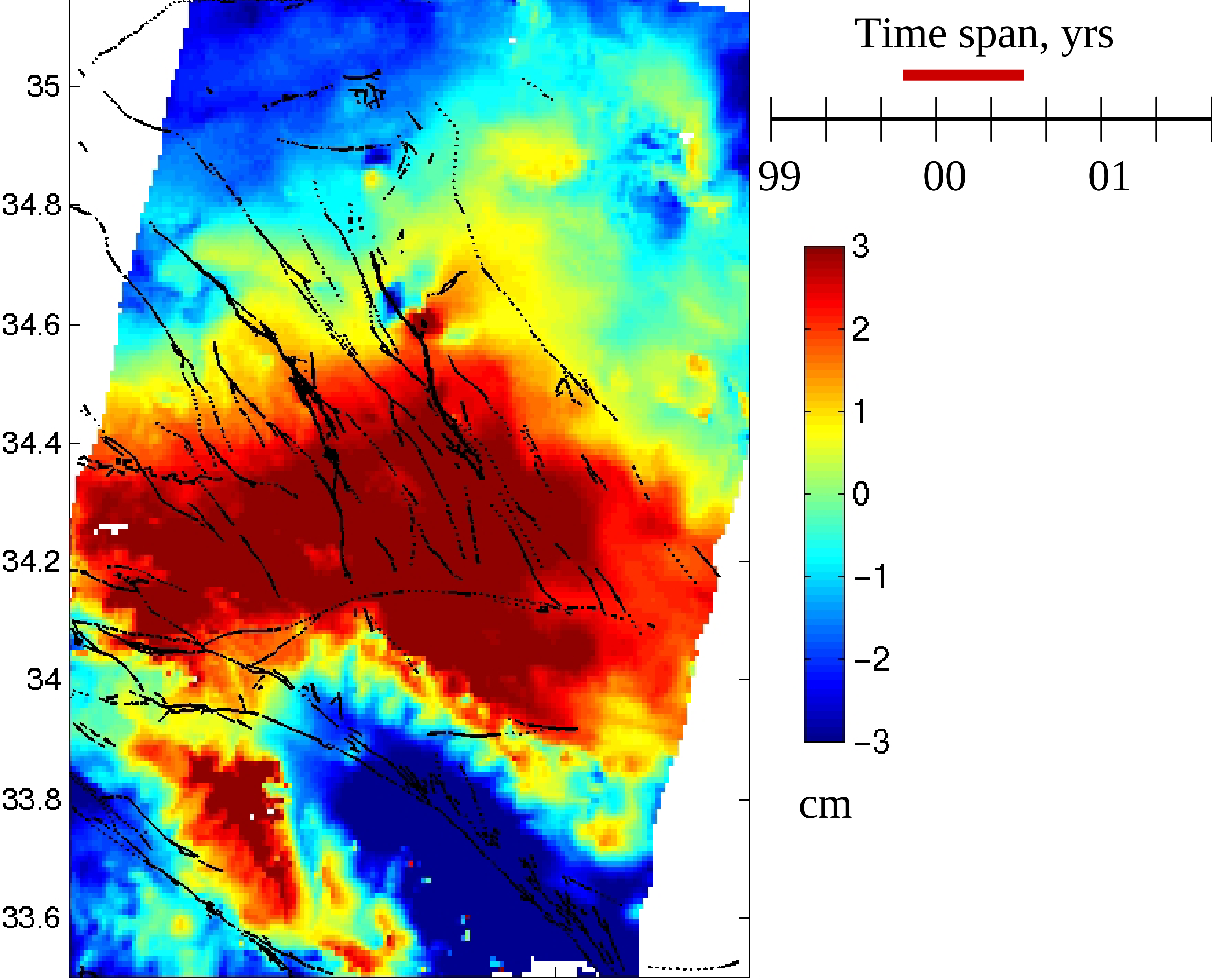

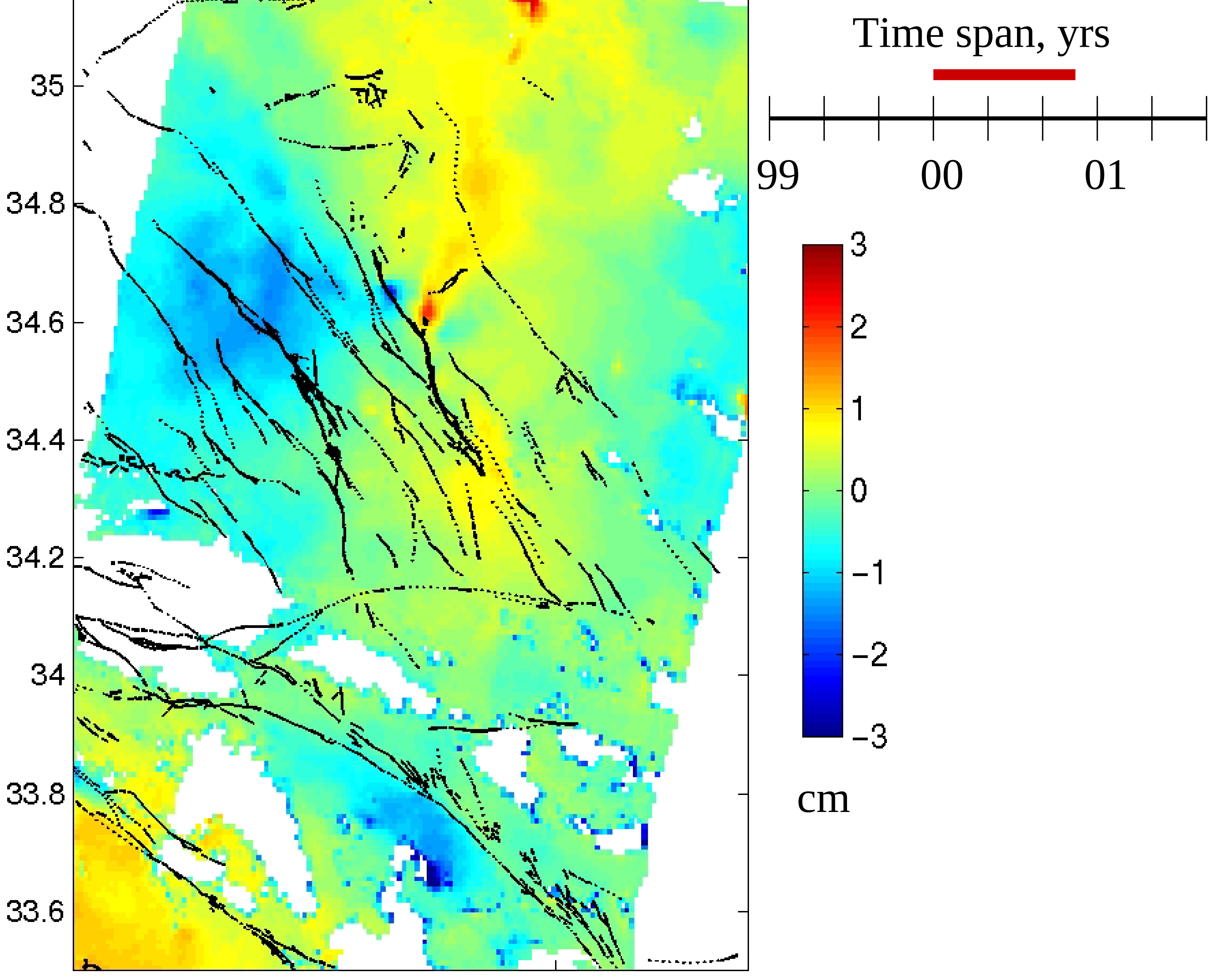

Time span, yrs
99
00
01
3
2
1
0
−1
−2
−3
cm
35
34.8
34.6
34.4
34.2
34
33.8
33.6

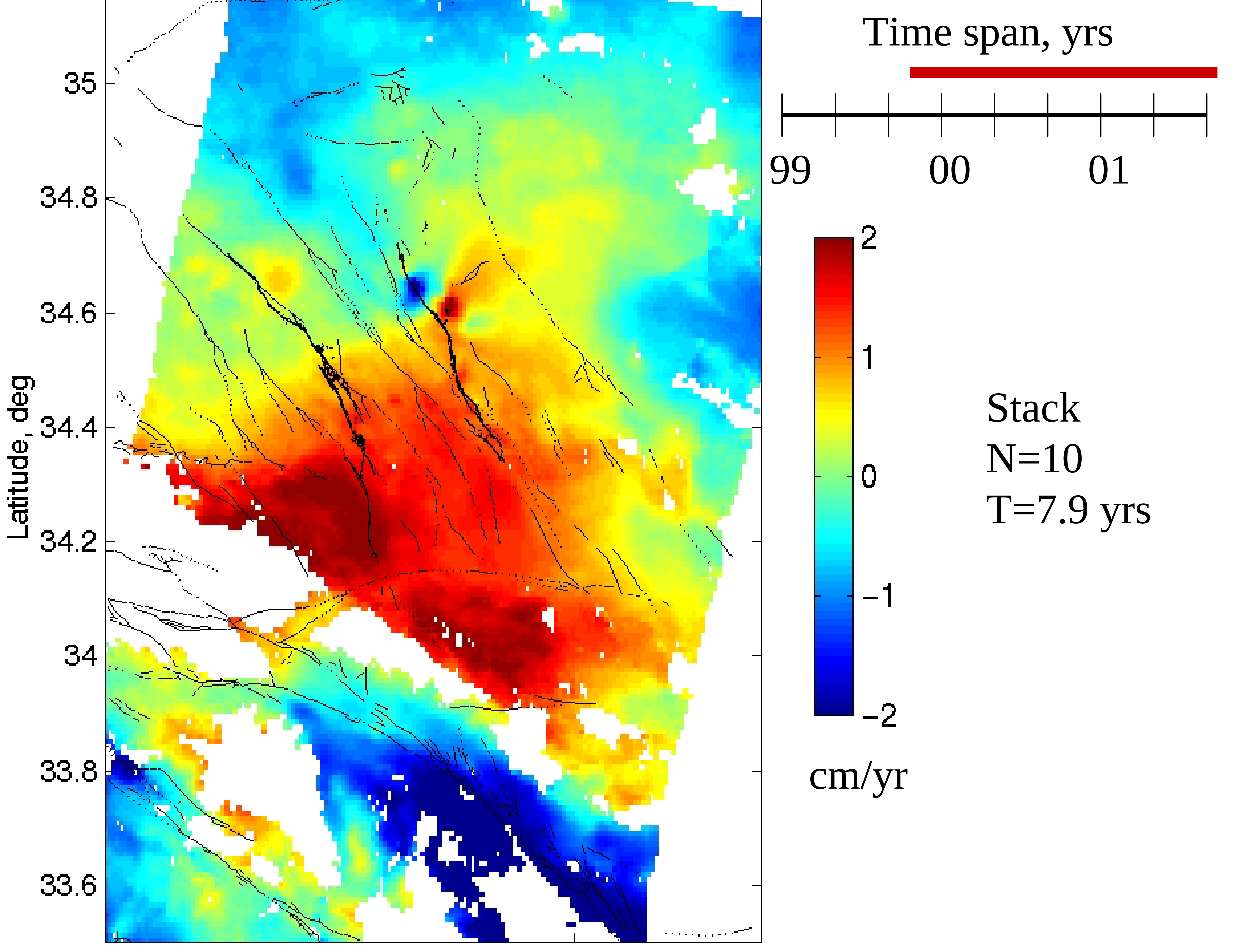
Time span, yrs
99
00
01
Latitude, deg
35
34.8
34.6
34.4
34.2
34
33.8
33.6
2
1
0
−1
−2
cm/yr
Stack
N=10
T=7.9 yrs

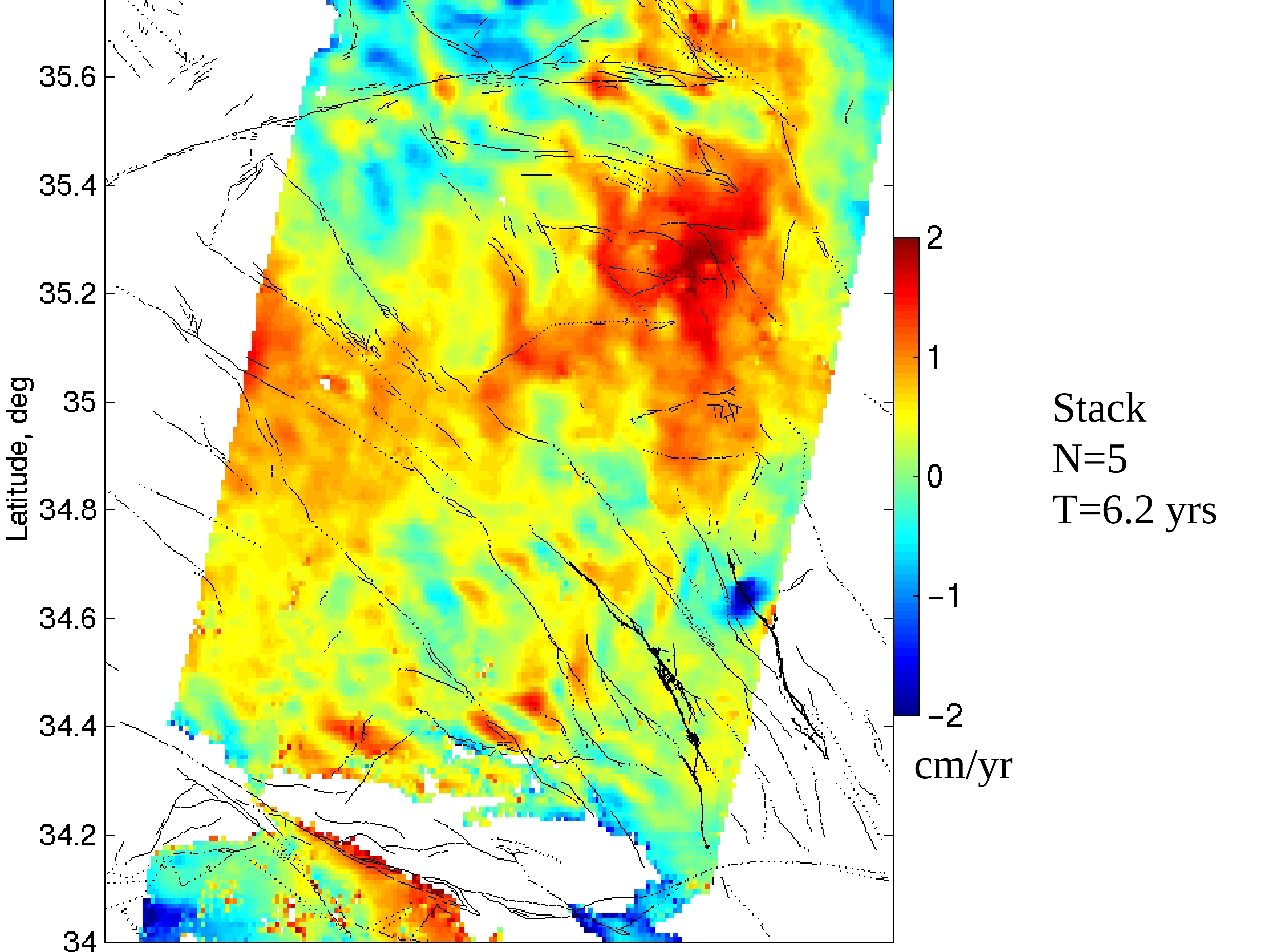
35.6
35.4
35.2
35
34.8
34.6
34.4
34.2
34
Latitude, deg
2
1
0
−1
−2
cm/yr
Stack
N=5
T=6.2 yrs

# Conclusions

- Given realistic rheologies, visco-elastic relaxation produces surface deformation that is very similar to that due to afterslip
- Post-seismic deformation transients following Landers and HM earthquakes lasted several years
- The kinetics of surface deformation measured with InSAR is consistent with hydraulic diffusivity of 0.1-1$m^2/s$; pore fluids are likely present throughout the seismogenic layer
- The post-seismic deformation observed after Landers and HM eqs is complex; a combination of “afterslip” and poro-elastic relaxation is required to explain the data

Savage et al., JGR 2003; Fialko, JGR 2004

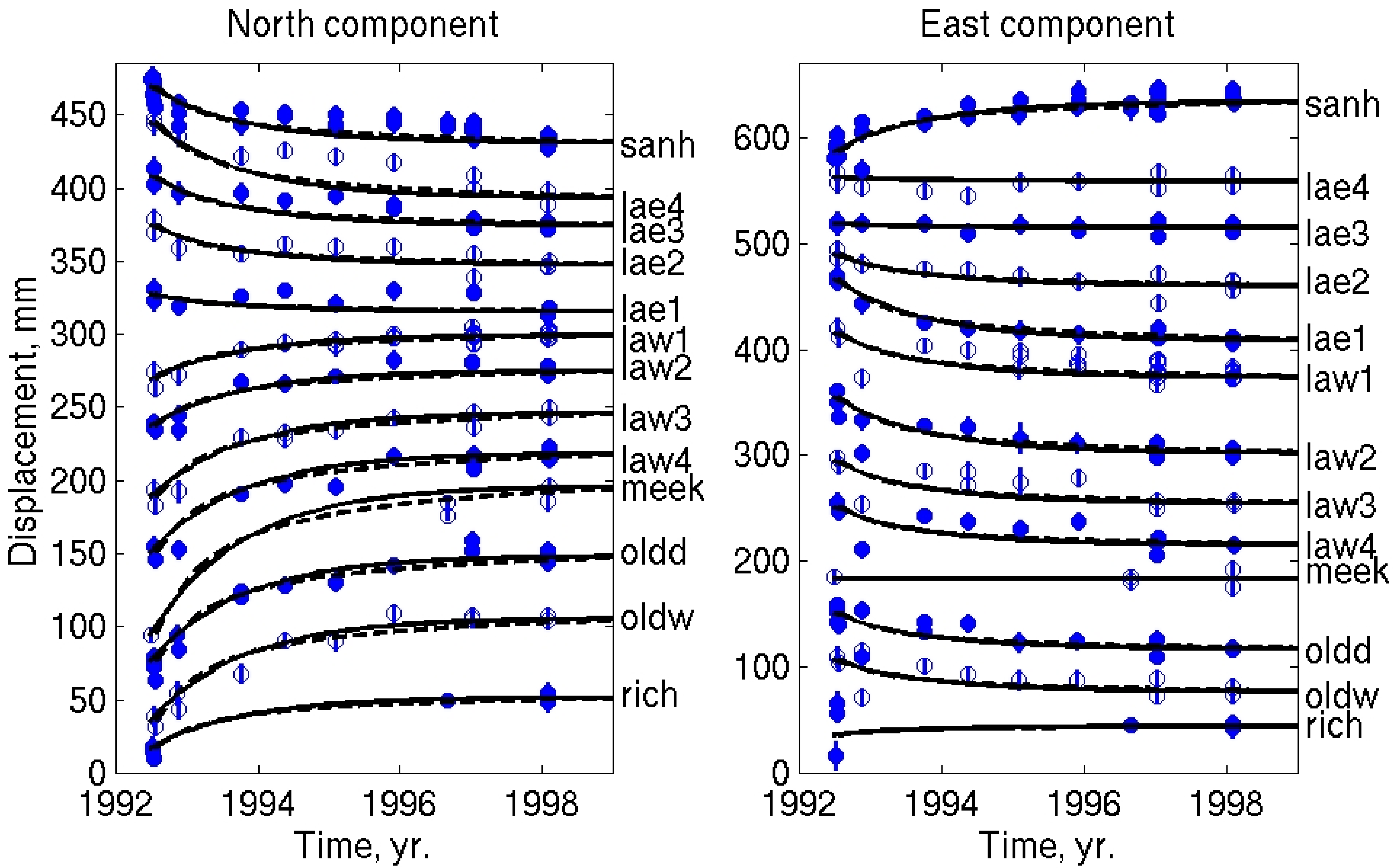

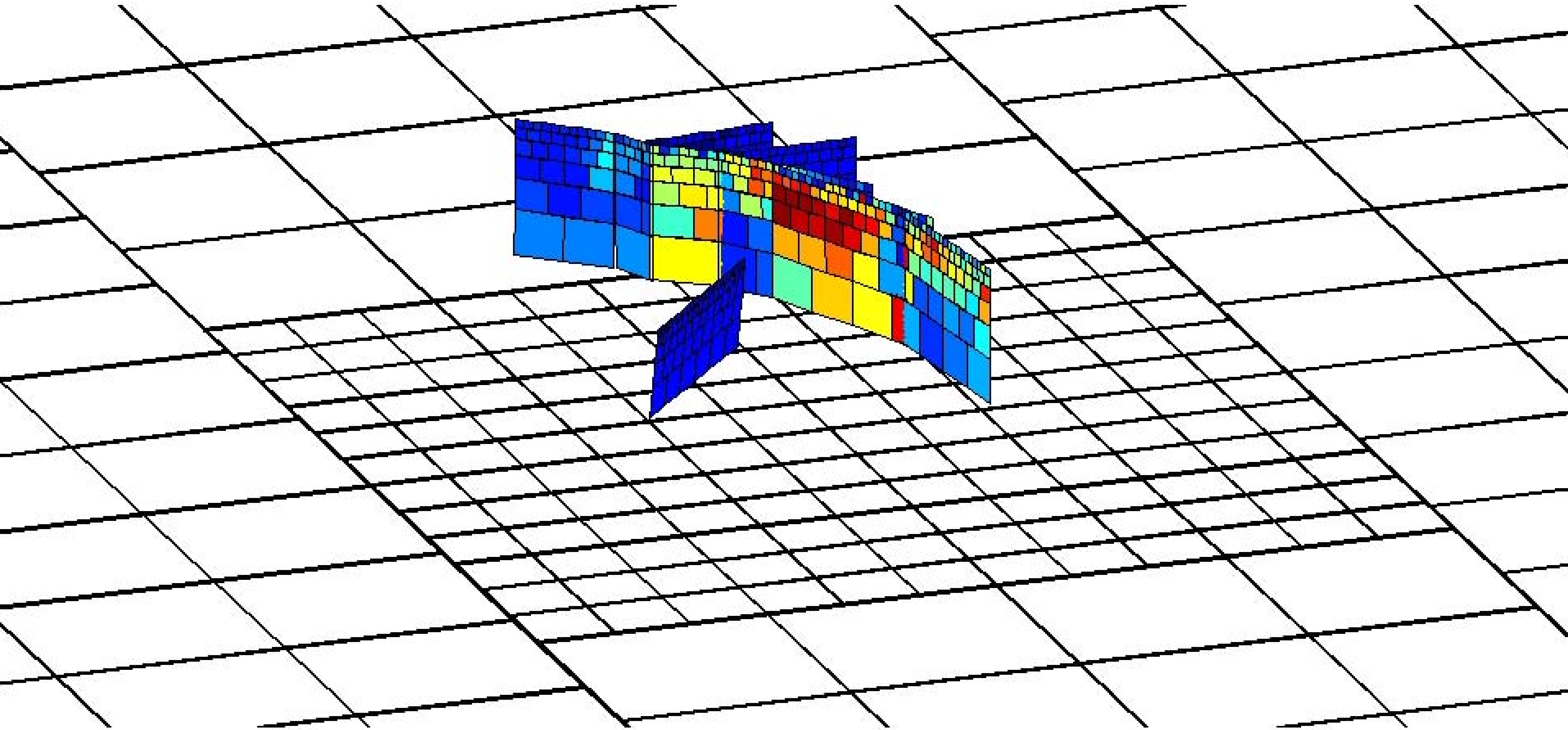

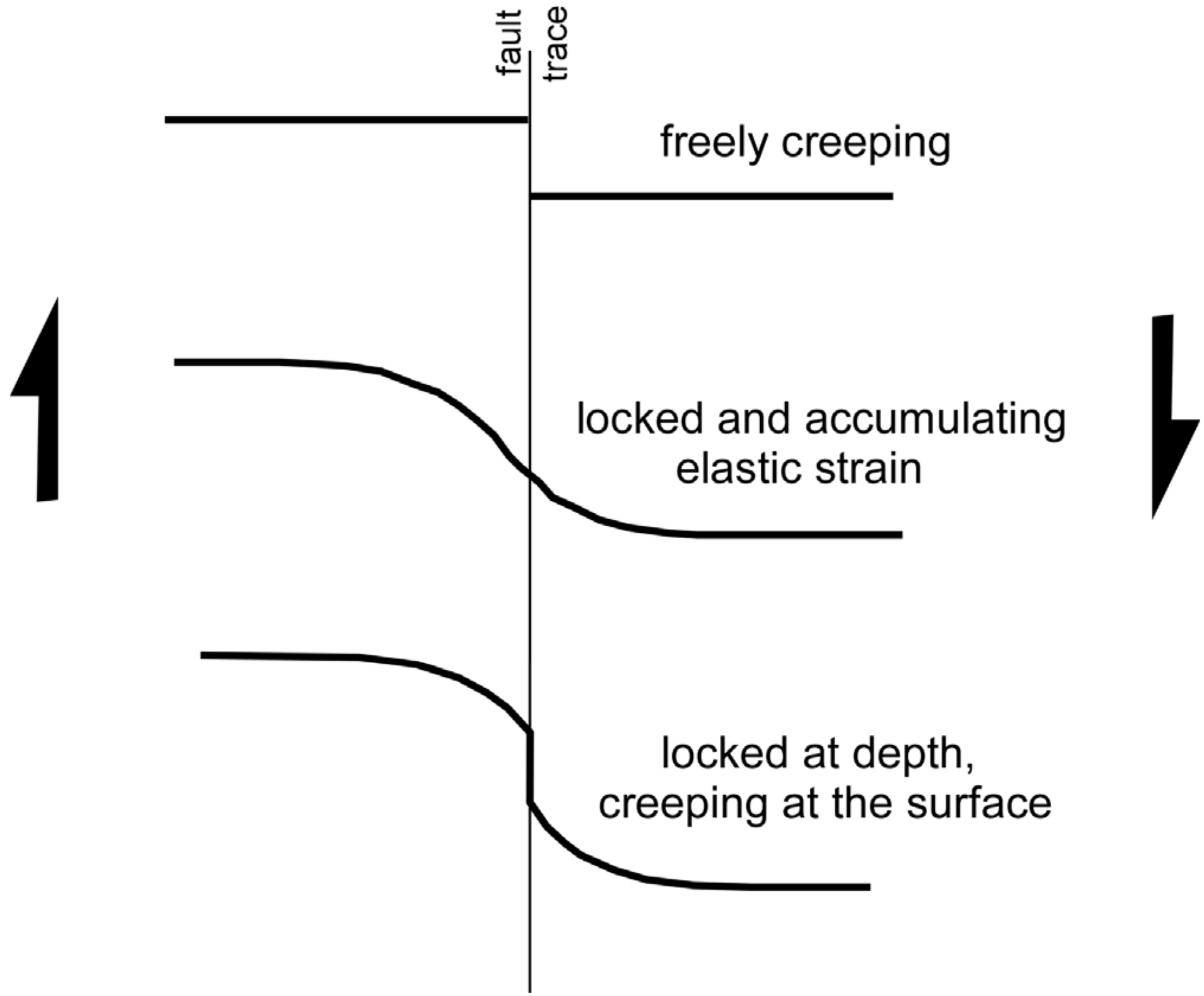

fault trace
freely creeping
locked and accumulating
elastic strain
locked at depth,
creeping at the surface

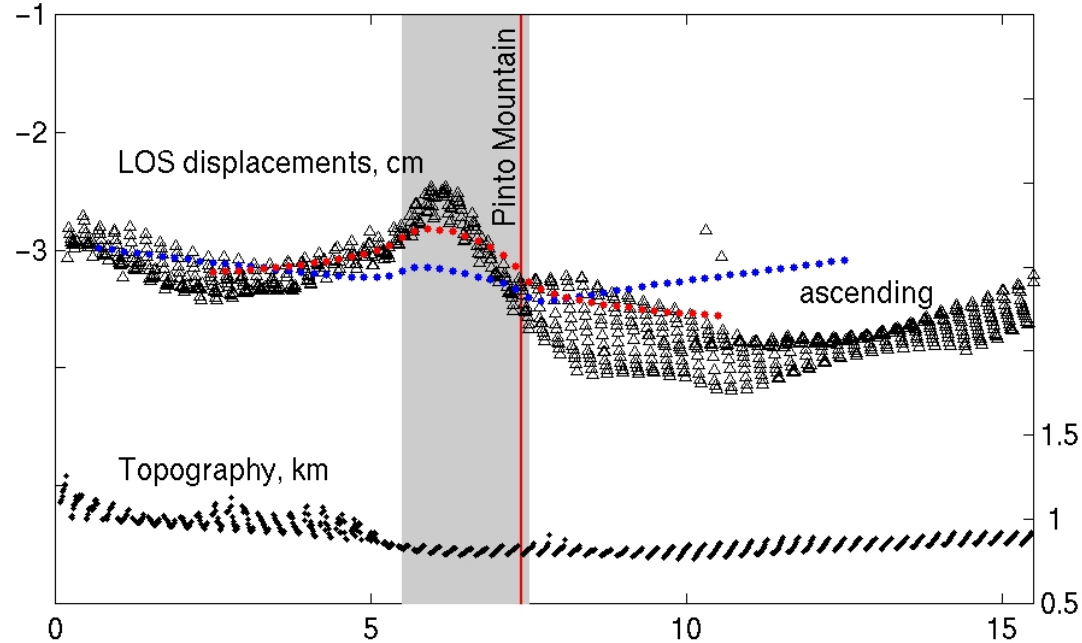


Landers co-seismic
(Fialko, JGR 2004)

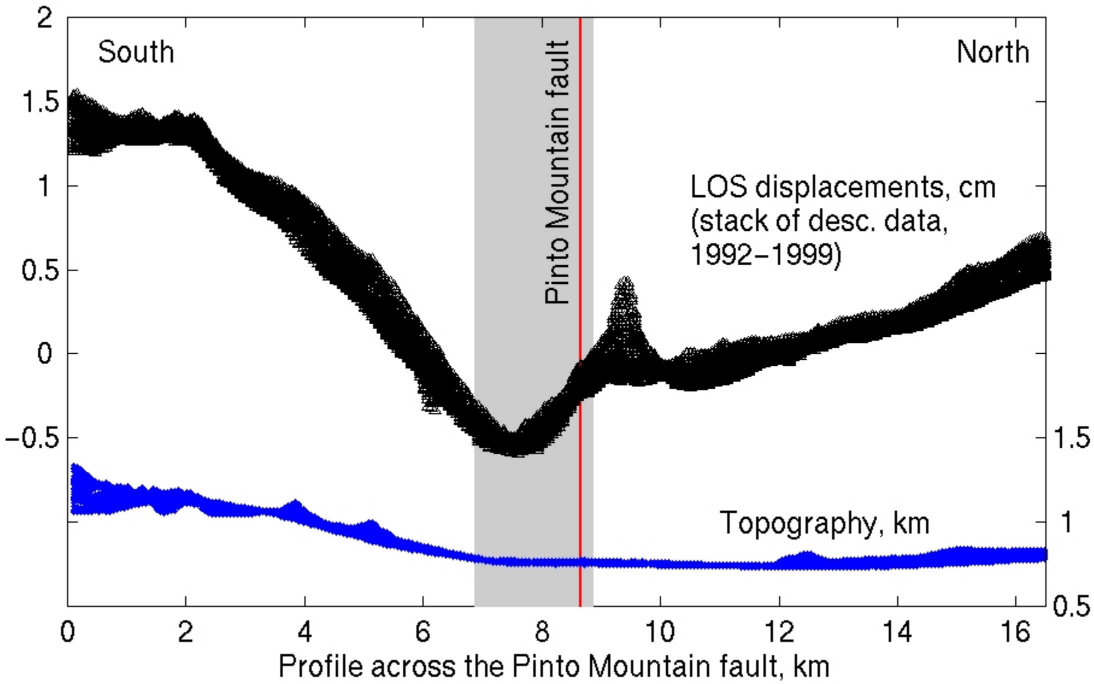


Post-Landers
deformation

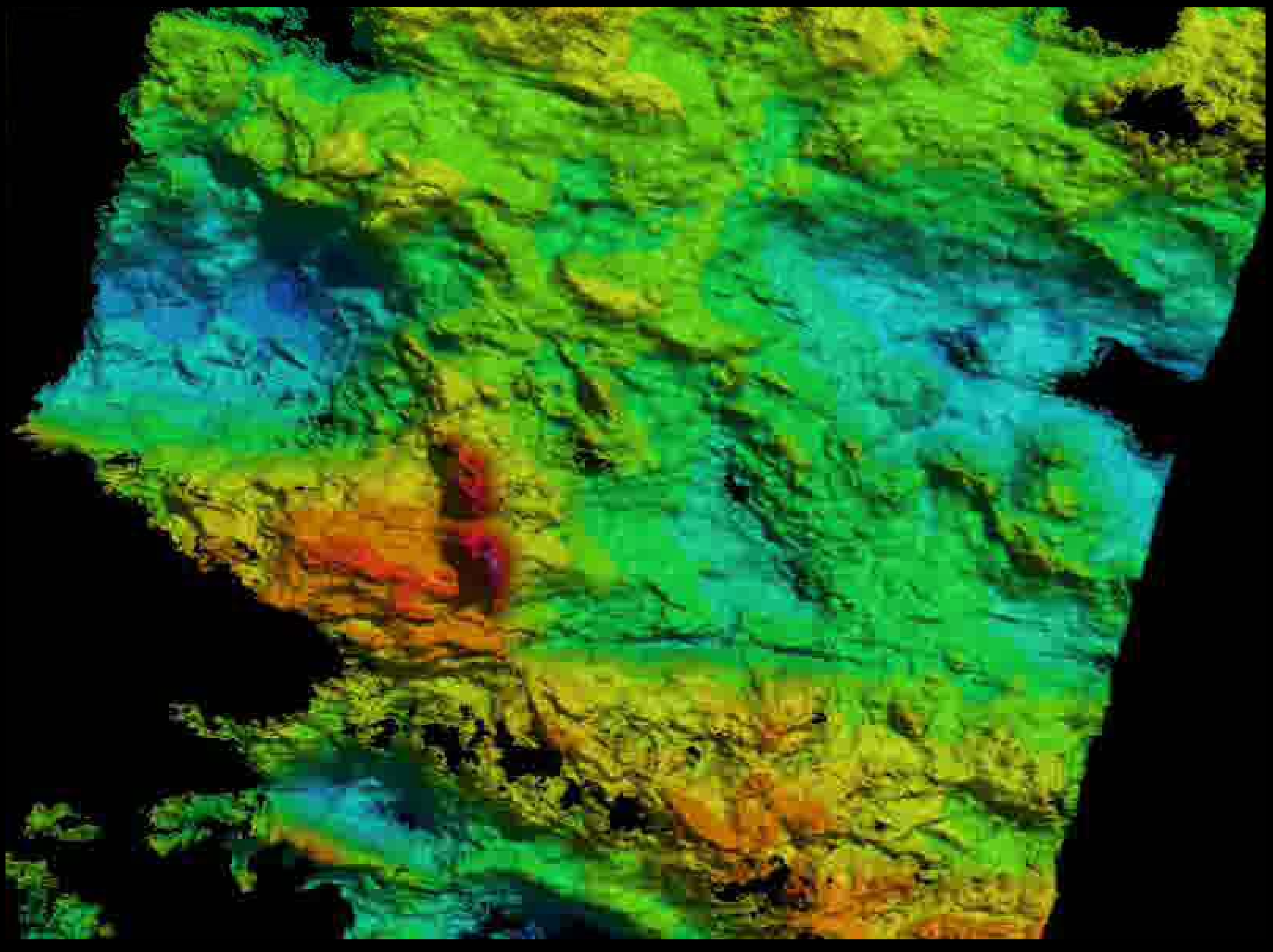

# Poro-elastic relaxation

2.5 km

15 km

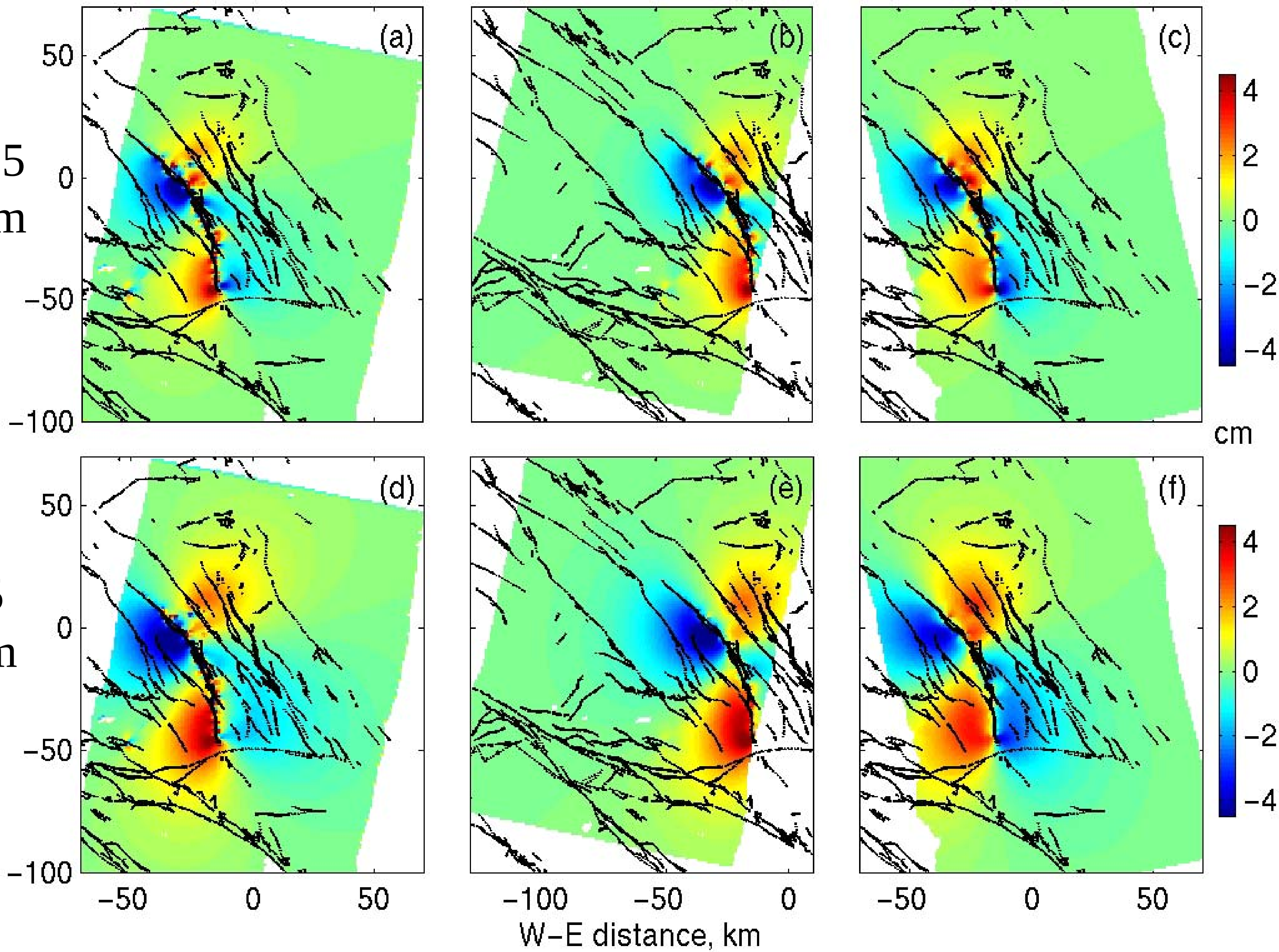

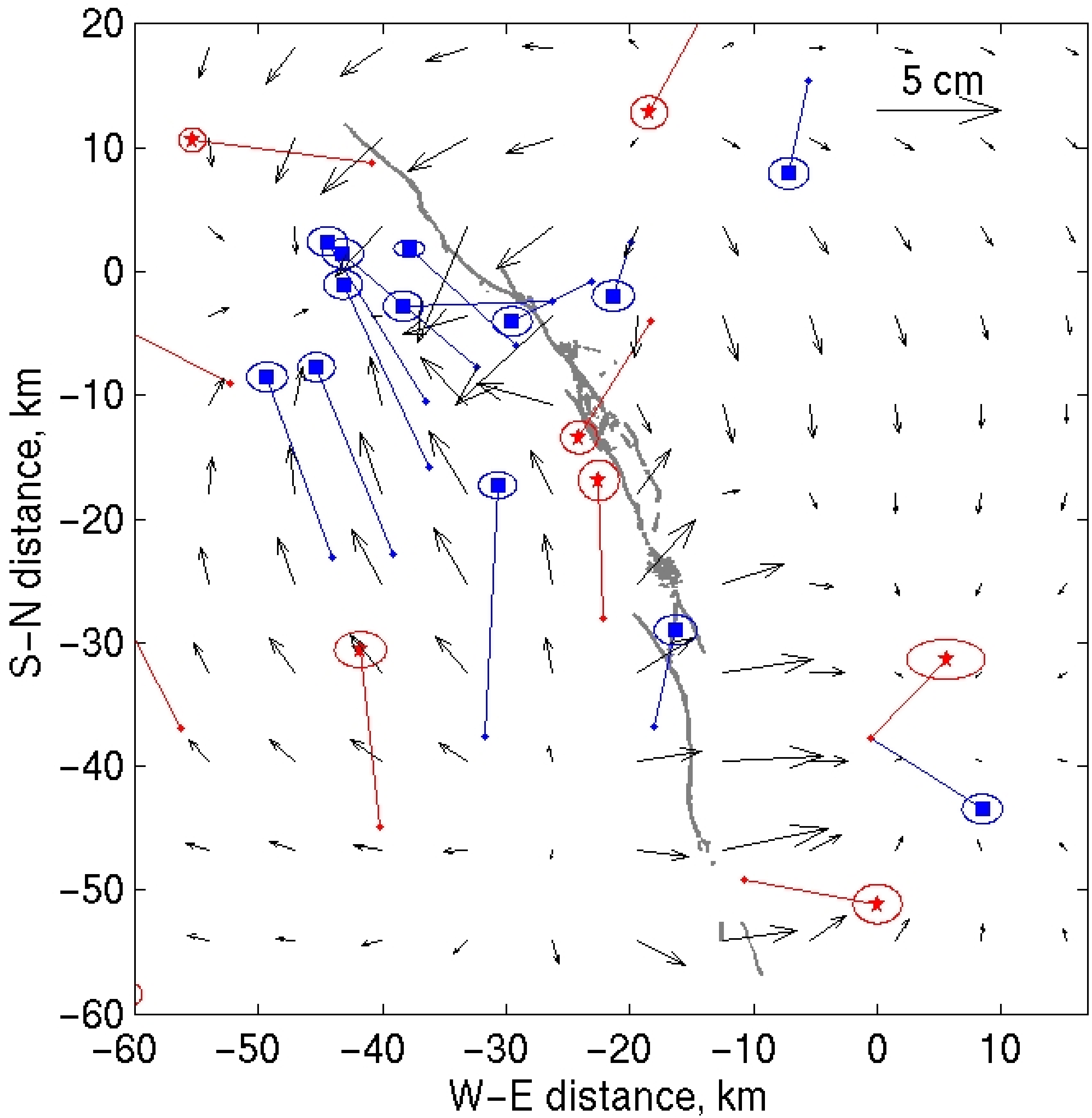
5 cm
S−N distance, km
W−E distance, km
20
10
0
−10
−20
−30
−40
−50
−60
−60
−50
−40
−30
−20
−10
0
10

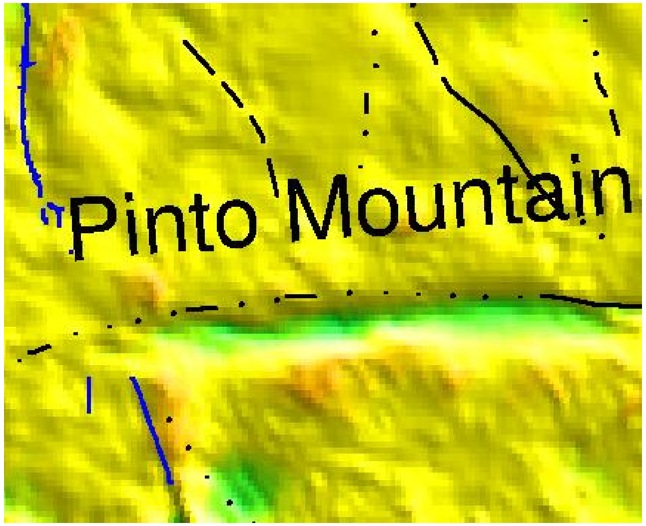
Pinto Mountain

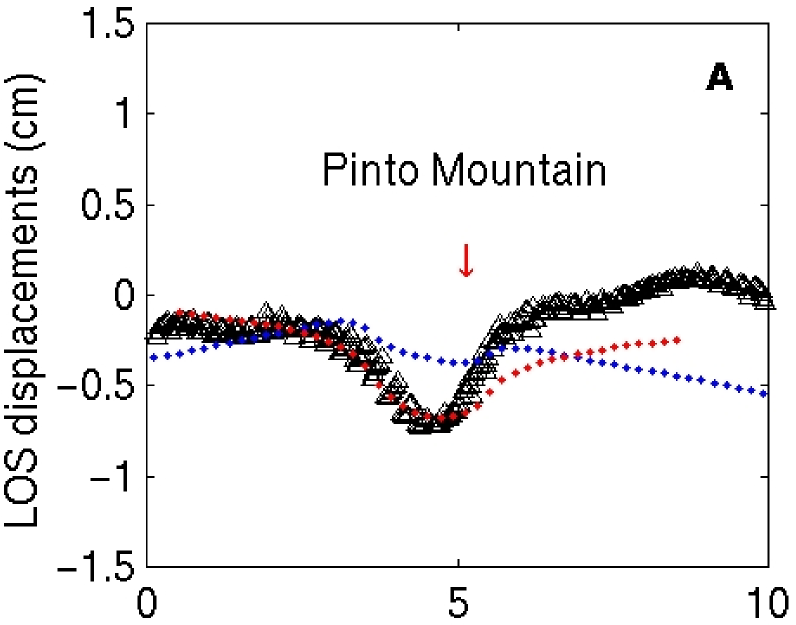
A
Pinto Mountain
LOS displacements (cm)
1.5
1
0.5
0
−0.5
−1
−1.5
0
5
10

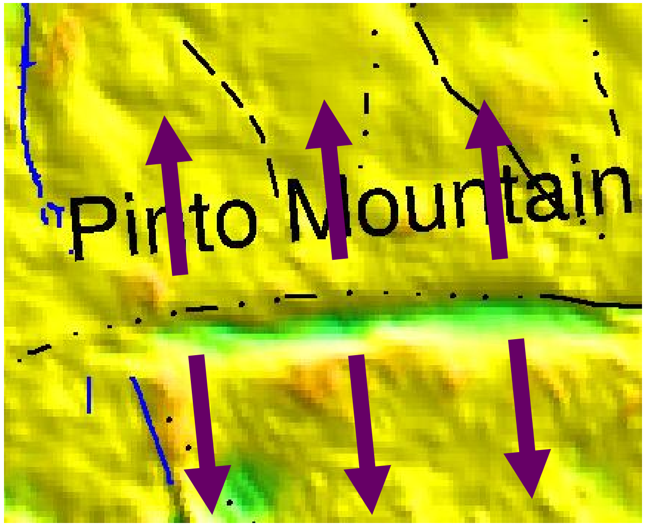
Pinto Mountain

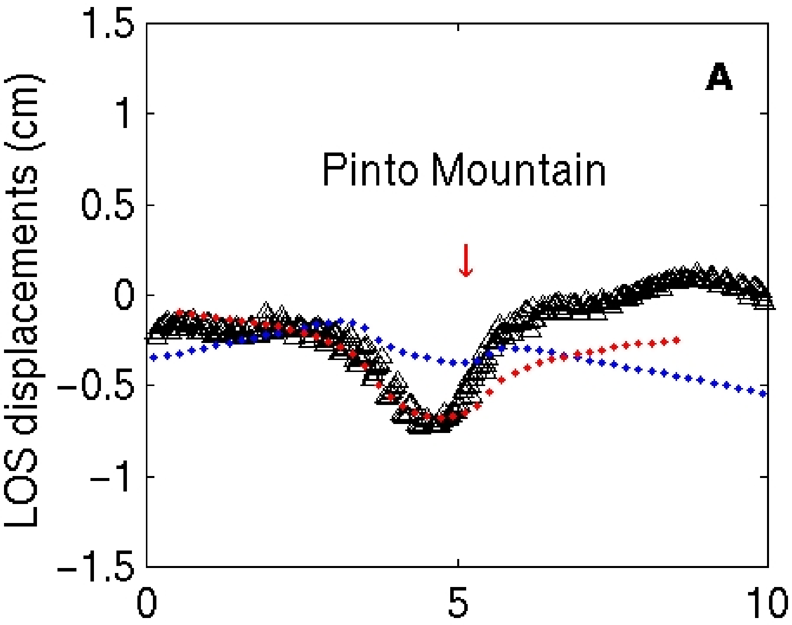
A
Pinto Mountain
LOS displacements (cm)
1.5
1
0.5
0
−0.5
−1
−1.5
0
5
10

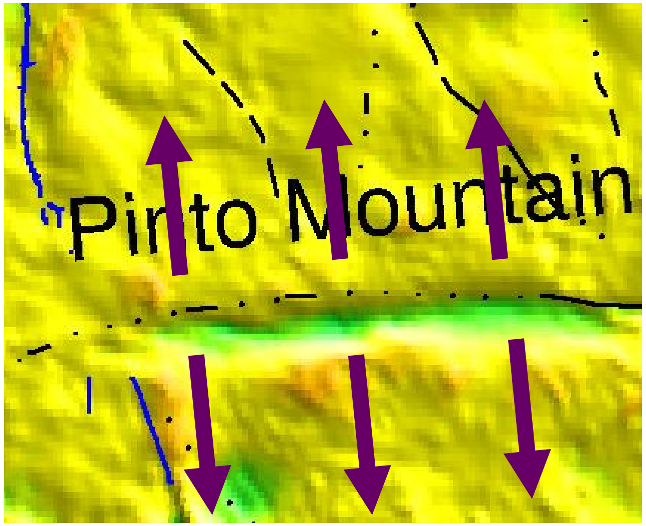
Pinto Mountain

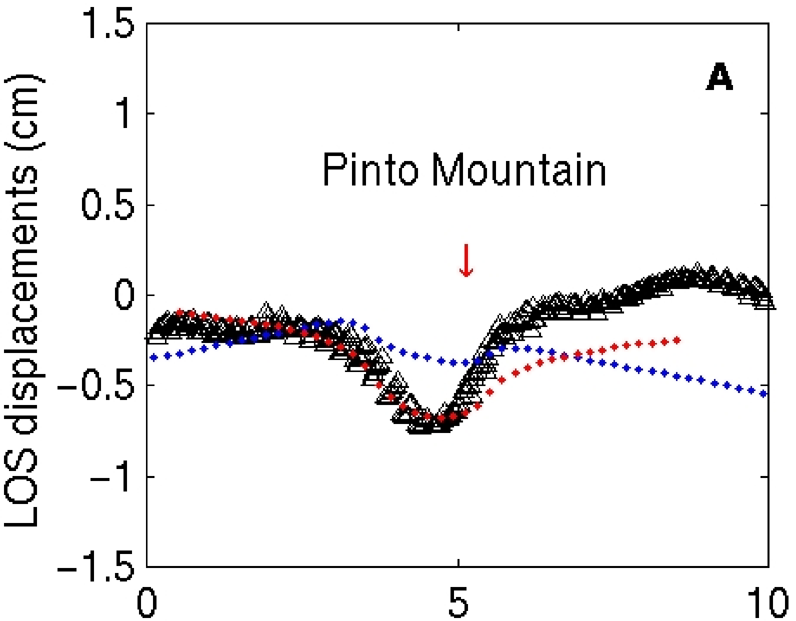
A
Pinto Mountain
LOS displacements (cm)
1.5
1
0.5
0
−0.5
−1
−1.5
0
5
10

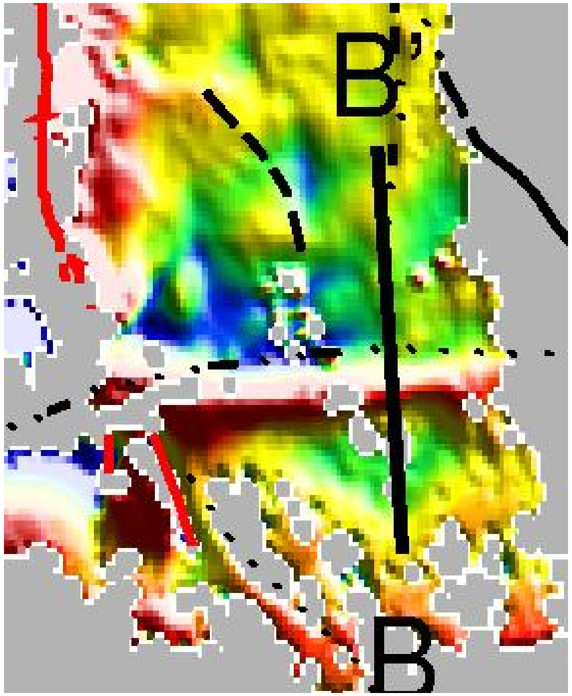
B'
B

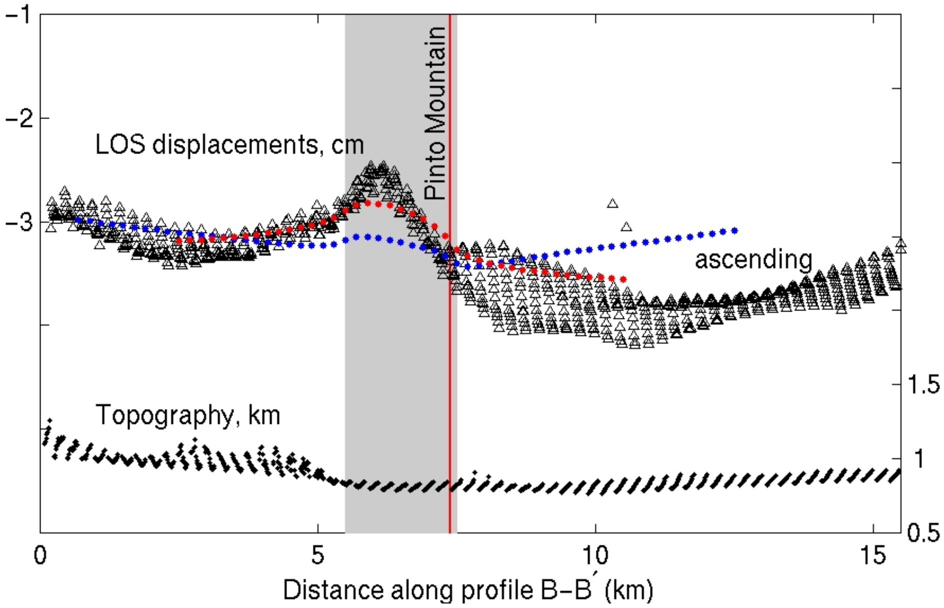
LOS displacements, cm
Pinto Mountain
ascending
Topography, km
−1
−2
−3
1.5
1
0.5
0
5
10
15
Distance along profile B−B′ (km)

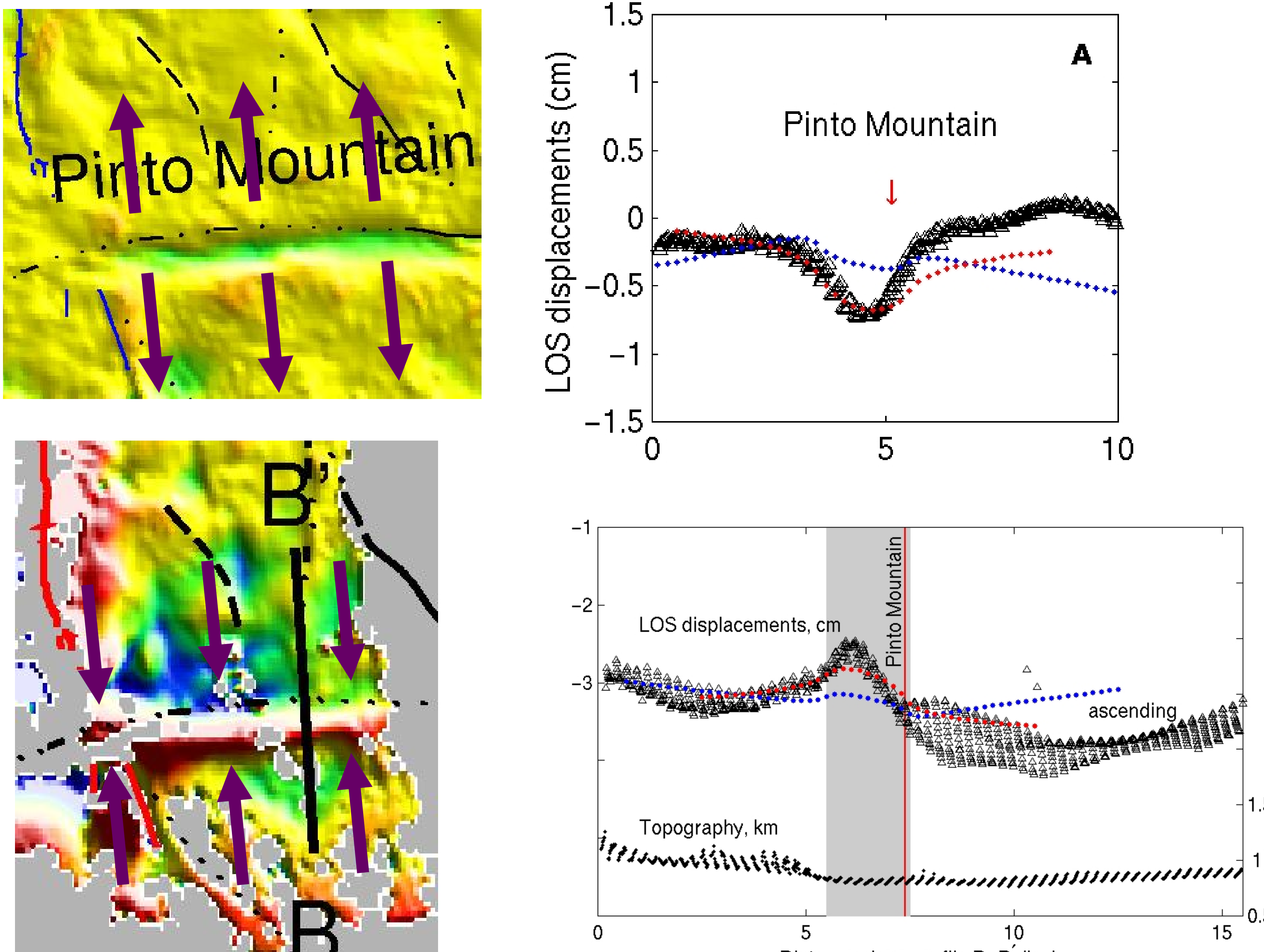

Pinto Mountain
B'
B
A
Pinto Mountain
LOS displacements (cm)
1.5
1
0.5
0
−0.5
−1
−1.5
0
5
10
Pinto Mountain
LOS displacements, cm
ascending
Topography, km
−1
−2
−3
1.5
1
0.5
0
5
10
15
Distance along profile B−B′ (km)

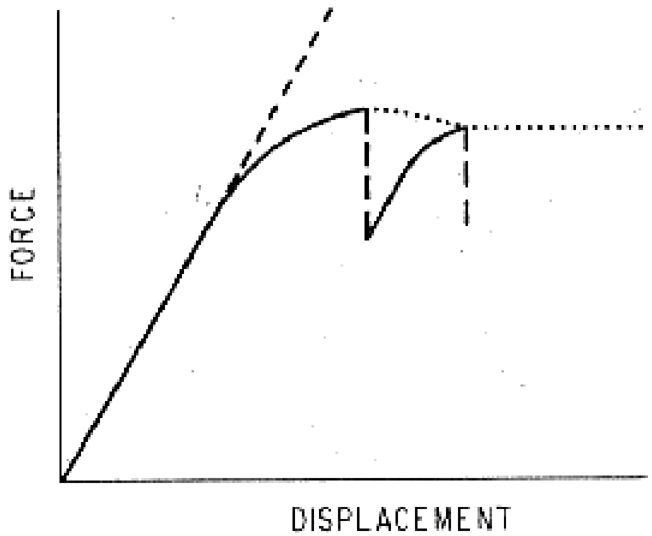
FORCE
DISPLACEMENT

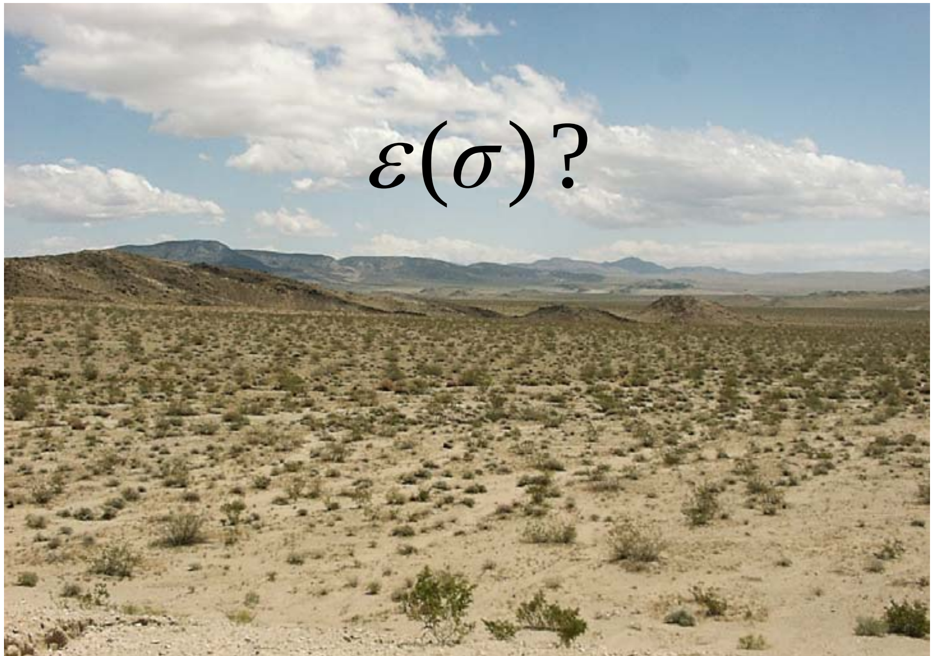
$\varepsilon(\sigma)$?

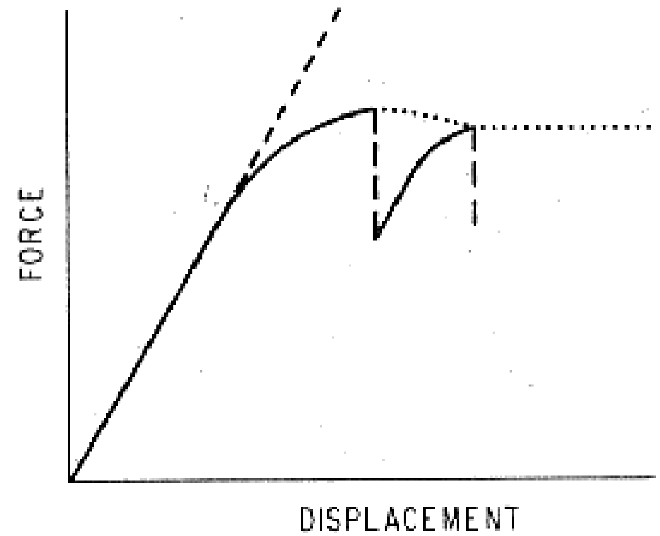


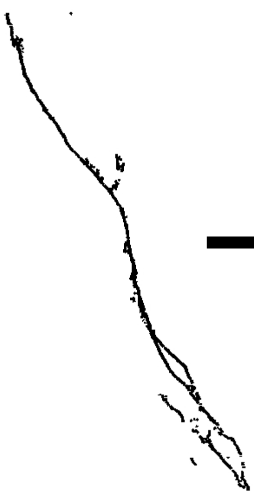

[redacted]

$$\varepsilon(t) = F(\sigma, E, t, D, \ldots)$$

[redacted]